Naval Oceanographic and
Atmospheric Research Laboratory

Technical Note 69
September 1990

XCTD Test: Reliability and Accuracy Study (XTRAS)

Z. R. Hallock
W. J. Teague
Oceanography Division
Ocean Science Directorate

These working papers were prepared for the timely dissemination of information; this document does not represent the official position of NOARL.

ABSTRACT

In May-June 1990 a test and evaluation of the newly developed XCTD (expendable conductivity, temperature, depth) probe was conducted in a region northeast of Barbados, where ideal conditions exist for such a test. Thirty-six XCTD probes were launched concurrently with nine CTD casts for intercomparison. The existing fall-rate equation (FRE) was found to be inadequate and new coefficients were computed by regression using the CTD data. After recalculating XCTD depths, simultaneous drops show significant probe-to-probe difference, indicating a nonsystematic difference in (primarily) the linear term in the FRE for each probe. Examination of temperature and conductivity shows a significant systematic offset of the XCTDs relative to the CTD, suggesting a calibration error. In addition, many of the probes exhibited huge, positive conductivity excursions indicative of conductivity cell malfunction. Sippican Ocean Systems has indicated that the cell malfunctions and the calibration problems are correctable, but it is not clear if there is a solution for the residual depth error.

ACKNOWLEDGMENTS

Sippican Ocean Systems participated in the field program and provided multiple acquisition systems for the expendables. Richard Myrick of Code 331 performed data acquisition and handled equipment logistics. H. Meyers, W. Stewart and S. Velasquez of NAVOCEANO provided valuable assistance with the operation. This research was funded by the Oceanographer of the Navy's (CNO OP-096) ASW Oceanography Program Office (NOARL Code 311) program elements 64704N and 63704N. The mention of commercial products or the use of company names does not in any way imply endorsement by the U.S. Navy or NOARL.

XCTD TEST: RELIABILITY AND ACCURACY STUDY (XTRAS)

INTRODUCTION

For a number of years the oceanographic community has been waiting for the market appearance of the expendable conductivity-temperature (XCTD) probe. Sippican Corporation has had this device under development since 1981. Prototype XCTDs have been field tested numerous times, with conductivity-cell problems occurring during each test. They recently developed a new design for the cell which avoids many of the problems they have encountered. A contract was let by the Naval Oceanographic and Atmospheric Research Laboratory (NOARL) to purchase 36 of these improved XCTD probes for an in-house test and evaluation (33 of the probes were a "flow-through" design, where water flows outside, as well as inside the conductivity cell; 3 were "foam filled" where an insulating layer of foam was placed around the cell to improve thermal response). This experiment eventually evolved into a joint effort between Sippican and NOARL, and was conducted during May and June 1990, aboard the USNS Lynch in an area about 280 nm northeast of Barbados. This region of the North Atlantic Ocean is unique in that between about 400 and 800 m depth, there exist quasi-permanent isothermal/isohaline step-like features which are ideal for testing vertical hydrographic profilers and expendable hydrographic probes. The reason for this is that a sequence of such stable, isothermal/isohaline layers separated by very thin (1-2 m thick) "sheets" (where gradients are large) allows the decoupling of sensor-calibration differences from errors in measured or inferred depth, when intercomparing instruments.

Upon leaving Fort Lauderdale, FL, USNS Lynch steamed toward a station near 16°N, 56°W (Figure 1), where historical data show that temperature (salinity) staircase structures exist. Within about 100 nm from station, expendable bathythermographs (XBTs) were launched every 30 nm. Spacing was decreased to 10 nm at 20 nm from station, and then reduced to 5 nm when staircase structures were found. At this point, the ship continued 4 nm farther and the structures disappeared. The ship then reversed course for about 6 nm and suitable structures were again found (i.e., about 10 to 15 distinct thermal steps in a vertical profile of temperature). The experiment then began. A 10 minute CTD time series at 4 m below the surface was first conducted to establish an absolute near-surface pressure calibration (and repeated later during the experiment). A deep CTD calibration cast to 3000 m was conducted, followed by a concurrent rapid-fire XBT survey (one T7 and three T5s launched simultaneously every 5 minutes for 1 hour). A CTD yo-yo cast to 1000 m and expendable tests commenced upon completion of the deep cast. CTD data were recorded on both down casts and up casts. XCTDs were dropped in simultaneous groups of four during the first nine CTD down casts. XCTD drops were timed such that the XCTD probes were concurrent with the CTD somewhere within the staircase structures.

DATA ACQUISITION AND PROCESSING

A Neil Brown Instrument System, Inc. (NBIS) Mark III CTD was used for profiling conductivity and temperature vs. pressure. Data were acquired at approximately 30 Hz as the CTD underwater unit was lowered at about 60 m/min. Data were recorded in full on nine-track digital tape and analog (audio) tape, and at about one sample per

meter on diskette. Salinities of water samples obtained with a rossette sampler were determined using a Guildline salinometer according to the practical salinity scale 1978 algorithm (Lewis, 1980). Salinities from the water samples collected at 3000 m from a single calibration cast were in exact agreement with the CTD. Final CTD data processing was performed at NOARL on the Code 331 VAX 11/750 computer. All data were processed from the nine-track digital tapes. Data processing included editing, calibrating, matching of temperature and conductivity response times, low-pass filtering and reducing to 1-m vertical levels and computing derived quantities (salinity, density, and depth). A three-point matching filter (Fofonoff et al., 1974) with a time constant of 60 msec was used to compensate for the difference in response time between temperature and conductivity sensors. Some salinity spiking still exists in strong gradient regions. Both raw and final processed data are stored in VFEB (VAX Fast and Easy Binary) format.

Expendable probe data were logged with Sippican's MK9 Digital Data Acquisition system. ASCII files containing raw temperatures and conductivities were supplied by Sippican. These data were likewise processed on the VAX 11/750 computer. Raw data and final processed data are stored in VFEB format.

GENERAL CHARACTERISTICS OF THE DATA

Figures 2-10 show a series of nine sets of temperature and conductivity profiles. Each set consists of a CTD cast plotted with four concurrent XCTD drops. XCTD drops were timed so that they would be virtually simultaneous with the CTD cast near 600 m depth, in the midst of the staircase structures. The maximum departure from simultaneity between CTD and XCTD was about 7 minutes, about 15-20% of the time interval between successive CTD downcasts; this occurred at the surface. The maximum depth error that could result from departure from simultaneity of CTD and XCTD is about 2.5 m, based on changes in feature depths from successive CTD downcasts. Hence, within an uncertainty of less than 2.5 m. each CTD cast together with its four XCTDs may be considered simultaneous. It is emphasized that 2.5 m is a maximum; for most of the features, especially in the staircase structures, the error is much less.

Several general observations can be made from Figures 2-10.

1. All profiles yield similar representations of the temperature/conductivity profile; the XCTD data appear somewhat noisier.

2. There are two "bad" XCTD drops: one in CTD group 7 (stops near 375 m) and one in group 11 (temperature calibration is bad).

3. There are numerous XCTD conductivity profiles that are offset over part or all of their domains to higher values, indicating a calibration problem or malfunction.

4. XCTDs show features consistently deeper than CTDs; This discrepancy appears to be depth dependent.

5. Considerable variability of feature depths is evident among simultaneous XCTDs. In particular, CTD group 10 (a worst case) shows a spread of about 20 m in the step region, well outside the manufacturer's specification. This variability appears to be dependent on depth.

6. Temperature calibration errors appear to be small relative to temperature offsets induced by the observed depth errors. Hence, XCTD-CTD temperature profile intercomparisons are not meaningful unless depth corrections are made.

From these observations we can infer that the existing fall-rate equation (FRE) is inadequate. Furthermore, a single set of FRE coefficients cannot remove all scatter seen in the depths of thermal features. We can also conclude that a significant problem exists with the conductivity measurements.

EVALUATION AND MODIFICATION OF THE FRE

The existing FRE for XCTDs (and XBTs, etc.) is of the form:

$$Z = At^2 + Bt \tag{1}$$

where Z is depth (m) and t is time (sec), and A and B are constant coefficients. Presently, $A = -4.95 \times 10^{-4} ms^{-2}$ and $B = 3.248 ms^{-1}$. The purpose of the following analyses is to evaluate the adequacy of this equation and to modify it as necessary. The evaluation/modification is based on comparisons of concurrent CTD and XCTD casts. In particular, the depths of robust, persistent features of the temperature profile are used as reference points with which to compare data.

For each CTD group a set of features in the temperature profiles which can be unequivocally identified were selected from two depth intervals: between the surface and about 200 m, and between 400 m and 700 m (steps). Larger-scale profile plots for these intervals for CTD group 10 appear in Figures 11a and b. In the deeper interval seven steps, corresponding to underlying layer temperatures of about 11.5, 10.8, 9.2, 8.7, 8.3, 7.9, and 7.6 °C, were selected due to their stability. These same steps were used for all CTD groups. For the shallow interval, feature selection was more difficult. While some CTD groups exhibited more useable features, six were selected for all groups to simplify analysis. Some of the features persisted throughout all groups but some were short lived. Features in this interval were selected at points where gradients changed abruptly, and at persistent minima and maxima, minimizing dependence on temperature accuracy. This procedure resulted in 13 features for each XCTD profile.

Hence, for each CTD group (i), we have $Z_{CTD}(i,j)$ for j=1,13 (CTD depth of feature) and $t_{XCTD}(i,j,k)$ for j=1,13; k=1,4 (XCTD time of feature), where j is the feature index and k is the index of the XCTD probe within the group (k ranges from 1 to 4 for 7 of the 9 groups; in 2 groups k_{max} is 3. due to defective XCTD probes).

A regression of Z_{CTD} on t_{XCTD} was performed to determine new FRE coefficients in the equation

$$Z = At^2 + Bt + C. \tag{2}$$

In particular, the analysis was conducted for five cases (I - A, B, C free; II - A fixed, B, C free; III - $A = 0, B, C$ free; IV - A, C fixed, B free; V - A fixed at mean of case I, method II, B, C free) and by two methods (I - regression averages over entire data set; II - regressions of individual XCTDs on corresponding CTDs) as follows.

Method I: Overall Regression

In this method within-group averages of the XCTD feature times were calculated as

$$\bar{t}_{XCTD}(i,j) = \frac{1}{k_{max}} \sum_{k=1}^{kmax} t_{XCTD}(i,j,k). \tag{3}$$

The regression of $Z_{CTD}(i,j)$ on $\bar{t}_{XCTD}(i,j)$, for $i = 1,9$ and $j = 1,13$, for a total of 117 members in the averages, was then performed for each of the five cases described above. The results of these calculations, together with RMS error, appear in Table 1. The first error is the error of the fit of $Z_{CTD}(i,j)$ on $\bar{t}_{XCTD}$. The second is the RMS difference between $Z_{CTD}(i,j)$ and $Z_{XCTD}(i,j,k)$. The latter error is considerably greater than the former, reflecting the within-group scatter of t_{XCTD}. In Figure 12 XCTD profiles for CTD group 10 are plotted after depths have been recalculated with the case-I coefficients.

Method II: Individual Regressions

In this method a determination of the regression coefficients was made for each XCTD. That is, the regression was $Z_{CTD}(i,j)$ on $t_{XCTD}(i,j,k)$ with averages computed over the 13 features (j) in each drop, yielding a total of 34 sets of coefficients, $A(i,k)$, $B(i,k)$, $C(i,k)$. These appear in Table 2 for case I. Their statistics, computed over the range of (i,k), for all cases, appear in Table 3. Also in Tables 2 and 3 are the ZA(1000) and ZB(1000); these are the contributions to the total depth due to coefficients A and B respectively, at the time to reach 1000 m at a nominal fall rate. This allows direct comparison of the effects of variations in the coefficients (note that C is already in the correct units). Figure 13 is similar to Figure 12 except that the individually calculated coefficients (Table 2) were used to recalculate depth. Cases II and V (not shown) produced virtually the same plots. Cases III and IV (also not shown) showed considerably worse agreement between XCTD and CTD.

DISCUSSION

It is clear from Figures 11 and 12 that calculating depth using a single set of coefficients (method I) removes the systematic offset which was evident with the original coefficients. Furthermore, a significant constant term of about -8 m appears, which was assumed to be zero in the original FRE. It is also clear, and expected, that the within-group scatter of feature depths is still present. One possible source of this scatter is launcher-acquisition system (LAS) specific errors. To check for this, averages (computed over the nine CTD groups) and standard deviations were calculated separately for data from each LAS (and also for CTDs as well) for the seven step features in the deep interval. These statistics are plotted in Figure 14. The generally deeper averages for the CTD data (relative to the XCTD data) are apparent. There is a systematic, negative offset of about 4 m for LAS 3 for most of the features. This offset is of questionable significance in the light of the temporal variability. It is clearly not large enough to explain the simultaneous probe scatter. Hence, most of the scatter must be due to probe- or drop-specific differences. In Figure 13 where depths have been calculated using the individually-determined coefficients (method II), virtually all the scatter has been removed, indicating that the quadratic form is adequate for a FRE. Very little additional scatter occurs during an individual drop. A significant decrease in overall error can be seen for this method on comparison of Tables 1 and 3. Table 2 shows that most of the variability in feature depths is accounted for in variations of the quadratic and linear terms (A and B), while variability in the constant term (C) is minimal. An examination of the variations in A and B shows a high, negative correlation (about -0.95) computed over the 34 drops, indicating that they are not independent. It can be shown that a process generated by a quadratic equation (e.g., eq. (2)) with fixed A and C but random fluctuations in B and random errors in the independent variable (t) can result in the observed negative correlation between the quadratic and linear coefficient estimates resulting from regression analysis. Hence, while the "real" quadratic coefficient might vary, the observed variation in case 1 is probably not meaningful. A value for A based on theory or overall statistics is, therefore, advisable, while B and C are allowed to vary. This leads us to case II which is essentially linear, with some additional terms based on the fixed value of A (a theoretical value supplied by Sippican). Case II, method II in Table 1 shows a diminished variability in B relative to case I; the overall error is slightly higher, but the analysis is more stable. The strictly linear case III is similar, with overall error again slightly greater. Case IV, on the other hand, shows a nearly doubling of the error (for method II); forcing the constant term to a prescribed value (as Sippican has done here) worsens the fit.

Since Case I yields the lowest total error it is reasonable to select the average value of

A found in that case (method II) and redo case II; this results in case V, which has overall error between those of cases I and II, but with the much-reduced standard deviation in B. The mode of the distribution of B is virtually equal to the average B for this case. Clearly, it is not practical (at this time) to propose individual sets of FRE coefficients. The best we can do is to choose the single set of average coefficients that minimizes overall error. The problem of the within-group scatter will still be present. We suggest, therefore, that a best estimate for an improved FRE is:

$$Z = -3.84 \times 10^{-4} t^2 + 3.19t - 7.91. \tag{4}$$

Two questions arise about the results of this analysis. What causes the apparent variability in the fall rate from probe-to-probe? What accounts for the offset of nearly 8 m? Answers to these questions are not known with certainty. There is some speculation that the variations in B may be the result of differences in probe weight and/or effective drag coefficient (A. W. Green, personal communication, 1984), the latter being the most likely cause. Many factors can affect the drag; for example, irregularities in probe surface, precession of the probe about its spin axis, variation of the friction of wire payout due to vertical shear of horizontal currents (this last, as well as other environmental factors such as water density, are not likely in this case since maximum scatter is seen with simultaneous probe drops). The second question may be a universal start-time offset (introduced by the LAS), initial probe acceleration near the surface or a constant depth error in the CTD data (this last could account for about 1/3 of the observed offset. Further studies of the existing data and, perhaps additional experiments, are needed to answer these questions satisfactorily.

TEMPERATURE AND CONDUCTIVITY CALIBRATION CHECK

Preparation of Data

The individually depth-corrected XCTD profiles and CTD profiles were interpolated to integral 1-meter levels. Differences ($DT = T_{CTD} - T_{XCTD}$, $DC = C_{CTD} - C_{XCTD}$) were formed at these levels. A sample of DT, DC (and DS) profile appears in Figure 15. The DT profile shows considerable noise and some rather large offsets in the upper 200 m. Most of this noise and offset are the result of residual depth errors. To avoid these errors, four relatively isothermal layers (one near 70 m and the others in the deep step interval) were selected for each CTD group. The depth limits of the selected layers appear in Table 4. These depth intervals were chosen to avoid vertical gradients as much as possible. The mean and standard deviation for each of these layers were computed for temperature and conductivity differences (DT and DC), and appear in Table 5. To better evaluate these statistics, standard deviation is plotted vs. mean in Figures 16, 17, and 18. A line through the origin corresponding to where the mean equals the standard deviation provides a significance bound for DT and DC. Different symbols denote points from different layers. The last three probes were of different construction (of the conductivity cell assembly) and are distinguished in the plots by a shaded symbol.

Temperature Errors

The uncertainty of the CTD temperatures are less than 0.003°C, as determined by laboratory and field calibrations. Hence, there is a mean offset of the XCTD temperatures

of 0.038°C with a scatter of about 0.002°C about that point (see Figure 16). The observed offset is well outside the manufacturer's (mfr's) tolerance and is also outside the standard deviation limit, indicating statistical significance. There seems to be no particular pattern with depth or probe type, suggesting a systematic error in the mfr's calibration procedure. If all DTs are shifted downward by the 0.038°offset, most points then fall within 0.03°of the origin, suggesting that if the calibration procedure is corrected, the temperatures will be marginally acceptable (4 of the 34 still fall outside the mfr's spec).

By the same procedure described above for the layer depths, an estimate of the effect of sampling-time difference yields a maximum error of 0.008°for the shallow layer (near 70 m) and 0.002°in the deep step interval; for most points, these errors are considerably smaller. This level of time-induced temperature error is not significant for these results.

Conductivity Errors

The uncertainty of CTD conductivities is less than 0.004 mS/cm. The much greater range of DC is illustrated by Figure 17. The large, negative values are indicative of a malfunction of the probes. On an expanded scale (Figure 18), a cluster of points between 0.02 and 0.04 mS/cm suggest the same calibration offset as that found for the temperature, excluding the obviously bad, negative points. Subsequent discussions with the mfr confirm that a calibration problem does exist for temperature and conductivity and that the large, negative DC values are probably the result of conductivity cell leaks resulting from cracks and/or separation of the potting compound around the cells. Another peculiarity exhibited in Figure 18 is the skewing of shallow-layer points to higher DC and standard deviation values. Time-induced error for the deep layers is not important for DC but may be a factor for the shallow layer. For CTD group 5, this error could be as high as 0.042 mS/cm, for group 8 it is 0.021 and for 11 it is 0.019. The remainder, however, are less than 0.006 in magnitude and two groups have negative offsets. Hence, time-induced error cannot explain all the observed clustering of points. Since the shallow layers are not nearly as close to being isothermal as the deep layers one might be tempted to invoke thermal lag to explain this skewing, but it is expected that DT should also exhibit a similar scatter, which it does not. At present, we have no good explanation for this effect.

If the leak problems of the conductivity cells as well as the problem with calibration procedures are corrected, the temperature and conductivity measuring accuracy of the XCTD will probably meet the cited values of ± 0.03°C and ± 0.03 mS/cm. Further, there does not seem to be a significant difference between the performance of the flow-through vs. the foam-filled XCTD.

CONCLUSIONS AND RECOMMENDATIONS

Of 36 XCTD probes dropped, 34 returned useful data for a nominal success rate of 94% (one of the failed probes was due to erroneous temperature calibration information stored in the probe). About 6 (18%) of the successful probes showed large, positive conductivity errors in the upper 200 m. This number increased to about 14 (41%) below about 500 m, indicating a malfunction in the conductivity cell. The remaining conductivities, as well as the temperatures, showed a systematic, negative offset of about 0.03 units relative to the CTD measurements, suggesting a problem with calibration procedures. These problems are probably correctable but, at present, the XCTD probes do not meet contractual specifications. An evaluation of the depth accuracy of the XCTD probe shows that a new set of coefficients, determined from the temperature data, significantly improves the fall-rate equation. However, intercomparisons of temperature profiles from simultaneously dropped

probes show nonsystematic, probe-to-probe depth differences as great as 5% of the depth, well outside the cited 2% accuracy. Further analysis reveals that these discrepancies are the result of some physical property of each probe, which affects its fall rate. Such properties include probe weight, volume, and factors influencing the effective hydrodynamic drag. Without further studies of probe dynamics, there is no obvious way to compensate for these effects in XCTD data. Furthermore, it is reasonable to speculate that this problem exists for other expendable probes. We recommend that the conductivity cell failures be addressed and the probe calibration procedures be improved. We also suggest that, until the fall rates of the probes can be made more uniform (or individual probe fall rates can be determined in the laboratory), the depth accuracy claimed by the manufacturer be modified to reflect these results.

REFERENCES

Fofonoff, N. P., S. P. Hayes, and R. D. Millard, Jr. (1974). WHOI/Neil Brown CTD Microprofiler: Methods of Calibration and Data Handling. Woods Hole Oceanographic Institution Technical Report, *WHOI 74-89*.

Green, A. W. (1984). Bulk Dynamics of the Expendable Bathythermograph (XBT). *Deep Sea Research 31(4)*, 415-426.

Lewis, E. L. (1980). The Practical Salinity Scale 1978 and its Antecedents, *IEEE, J. Oceanic Eng., Vol. OE-5*, 3-8.

Table 1: Fall-rate equation coefficients (A,B,C) computed by regression, of CTD depths on XCTD times,over all probes and features (Method-I). E1 is error of fit, E2 is overall RMS difference between feature depths from CTD and XCTDs.

	A	B	C	E1	E2
Case-I	-3.67E-04	3.19	-7,79	2.43	4.14
Case-II	-5.33E-04	3.22	-8.59	2.49	3.99
Case-III	-0-	3.11	-6.05	2.63	4.60
Case-IV	-5.33E-04	3.20	-4.80	3.03	5.09
Case-V	-3.84E-04	3.19	-7.88	2.45	4.12

Table 2: Method-II, Case-I; individually-determined regression coefficients with A, B, C free. Zs and C are in meters, A in ms^{-2}, B in ms^{-1}. The last four columns are the contributions to total depth by the quadratic (A) and linear (B) terms (e.g. ZA-1000 is the contribution of the term At(1000), where t(1000) is the time for the probe to reach 1000 m at a nominal, constant fall-rate).

CTD			A	B	C	ZA-500	ZA-1000	ZB-500	ZB-1000
1	1	1	-.2699E-03	3.180	-6.	-7.	-28.	509.	1018.
2	1	2	-.3888E-03	3.174	-6.	-10.	-40.	508.	1016.
3	1	3	-.4102E-03	3.211	-6.	-11.	-42.	514.	1028.
4	1	4	-.3909E-03	3.183	-7.	-10.	-40.	509.	1019.
5	2	1	-.6405E-03	3.259	-7.	-16.	-66.	521.	1043.
6	2	2	-.4485E-03	3.230	-7.	-11.	-46.	517.	1034.
7	2	3	-.4334E-03	3.228	-7.	-11.	-44.	517.	1033.
8	2	4	-.6709E-03	3.261	-8.	-17.	-69.	522.	1044.
9	3	1	-.4238E-03	3.206	-9.	-11.	-43.	513.	1026.
10	3	2	-.7207E-03	3.296	-9.	-18.	-74.	527.	1055.
11	3	3	-.5459E-03	3.226	-9.	-14.	-56.	516.	1032.
12	3	4	-.5735E-03	3.243	-10.	-15.	-59.	519.	1038.
13	4	1	-.3645E-03	3.186	-7.	-9.	-37.	510.	1020.
14	4	2	-.3581E-03	3.189	-7.	-9.	-37.	510.	1021.
0	4	3	-.5808E-04	0.189	0.	-1.	-6.	30.	61.
15	4	4	-.3170E-03	3.196	-4.	-8.	-32.	511.	1023.
16	5	1	-.4264E-03	3.203	-9.	-11.	-44.	512.	1025.
17	5	2	-.3418E-03	3.197	-9.	-9.	-35.	512.	1023.
18	5	3	-.7144E-03	3.308	-9.	-18.	-73.	529.	1059.
19	5	4	-.5491E-04	3.093	-8.	-1.	-6.	495.	990.
20	6	1	-.5465E-03	3.235	-10.	-14.	-56.	518.	1035.
21	6	2	-.3134E-03	3.165	-8.	-8.	-32.	506.	1013.
22	6	3	-.4809E-03	3.174	-10.	-12.	-49.	508.	1016.
23	6	4	-.3958E-03	3.223	-9.	-10.	-41.	516.	1031.
24	7	1	-.1039E-03	3.101	-7.	-3.	-11.	496.	992.
25	7	2	-.1870E-04	3.053	-7.	0.	-2.	488.	977.
26	7	3	-.4425E-03	3.219	-8.	-11.	-45.	515.	1030.
27	7	4	-.4949E-03	3.254	-10.	-13.	-51.	521.	1041.
0	8	1	-.5808E-04	0.189	0.	-1.	-6.	30.	61.
28	8	2	-.7356E-04	3.133	-8.	-2.	-8.	501.	1003.
29	8	3	-.4824E-03	3.216	-7.	-12.	-49.	515.	1029.
30	8	4	-.1099E-03	3.120	-6.	-3.	-11.	499.	998.
31	9	1	-.1615E-03	3.143	-10.	-4.	-17.	503.	1006.
32	9	2	-.3357E-03	3.141	-8.	-9.	-34.	503.	1005.
33	9	3	-.2855E-03	3.170	-7.	-7.	-29.	507.	1014.
34	9	4	-.3260E-03	3.141	-8.	-8.	-33.	503.	1005.

Table 3: Average fall-rate equation coefficients computed by regression, of individual-probe CTD depths on XCTD times (method-II). ZA-1000, ZB-1000 are contributions to total depth by terms A, B. E is overall error of the fit.

	A	B	C	ZA-1000	ZB-1000	E
Case-I	-3.84±1.81E-04	3.19±.06	-7.89±1.41	-39.35±18.58	1022±18	1.33
Case-II	-5.33E-04	3.22±.03	-8.62±1.36	-54.58	1032±8	1.59
Case-III	-0-	3.11±.03	-6.08±1.32	0	997±8	1.88
Case-IV	-5.33E-04	3.20±.03	-4.80	-54.58	1024±9	3.03
Case-V	-3.84E-04	3.19±.02	-7.91	-39.32	1022±8	1.53

Table 4: Selected near-isothermal layer depth limits (m)

	Layer-1	Layer-2	Layer-3	Layer-4
CTD-4	60-80	462-484	583-598	613-627
CTD-5	62-82	458-474	581-598	608-622
CTD-6	60-80	445-471	576-592	604-615
CTD-7	60-80	442-463	583-592	602-616
CTD-8	45-65	441-460	579-588	600-616
CTD-9	50-70	452-463	554-568	600-611
CTD-10	50-70	418-435	554-572	616-626
CTD-11	60-80	426-441	554-567	576-586
CTD-12	60-80	422-445	552-565	605-616

Table 5a: Means and standard deviations of temperature error (DT) for layers defined in Table 4.

Temperature

		DEPTH-1		DEPTH-2		DEPTH-3		DEPTH-4		VERT. AV	
C	X	AV	SD	AV	SD	AV	SD	AV	SD	AV	SD
4	1	0.027	0.045	0.041	0.036	0.016	0.021	0.044	0.015	0.032	0.031
4	2	0.036	0.039	0.056	0.032	0.041	0.009	0.050	0.010	0.046	0.026
4	3	0.034	0.037	0.039	0.026	0.024	0.014	0.053	0.022	0.037	0.026
4	4	0.056	0.033	0.060	0.031	0.035	0.023	0.046	0.029	0.049	0.029
5	1	0.040	0.028	0.035	0.015	0.033	0.022	0.024	0.026	0.033	0.023
5	2	0.032	0.022	0.033	0.025	0.043	0.026	0.046	0.027	0.039	0.025
5	3	0.041	0.025	0.034	0.013	0.035	0.012	0.055	0.024	0.041	0.020
5	4	0.025	0.030	0.034	0.012	0.047	0.012	0.042	0.027	0.037	0.022
6	1	0.051	0.013	0.037	0.016	0.050	0.026	0.056	0.017	0.049	0.019
6	2	0.046	0.019	0.033	0.025	0.031	0.029	0.031	0.021	0.035	0.024
6	3	0.033	0.036	0.041	0.015	0.022	0.013	0.041	0.018	0.035	0.023
6	4	0.063	0.021	0.041	0.026	0.045	0.032	0.030	0.010	0.045	0.024
7	1	0.034	0.017	0.028	0.022	0.032	0.013	0.046	0.019	0.035	0.018
7	2	0.067	0.026	0.042	0.021	0.053	0.011	0.042	0.022	0.051	0.021
7	4	0.046	0.019	0.029	0.020	0.029	0.015	0.023	0.015	0.032	0.017
8	1	0.017	0.031	0.029	0.027	0.049	0.009	0.053	0.015	0.037	0.022
8	2	0.022	0.025	0.025	0.028	0.049	0.014	0.033	0.012	0.032	0.021
8	3	0.018	0.033	0.027	0.021	0.050	0.022	0.033	0.011	0.032	0.023
8	4	0.032	0.032	0.032	0.037	0.050	0.028	0.056	0.017	0.043	0.029
9	1	0.044	0.019	0.073	0.015	0.059	0.010	0.054	0.008	0.057	0.014
9	2	0.021	0.014	0.043	0.013	0.033	0.017	0.047	0.013	0.036	0.014
9	3	0.025	0.034	0.034	0.018	0.029	0.022	0.009	0.037	0.024	0.029
9	4	0.019	0.022	0.039	0.015	0.035	0.018	0.033	0.029	0.032	0.022
10	1	0.027	0.020	0.039	0.014	0.043	0.007	0.042	0.020	0.038	0.016
10	2	0.031	0.031	0.039	0.020	0.033	0.020	0.036	0.021	0.035	0.023
10	3	0.017	0.028	0.024	0.015	0.023	0.010	0.029	0.029	0.023	0.022
10	4	0.038	0.016	0.040	0.030	0.037	0.037	0.043	0.019	0.039	0.027
11	2	0.032	0.028	0.051	0.007	0.043	0.012	0.035	0.017	0.040	0.018
11	3	0.042	0.019	0.044	0.019	0.036	0.010	0.019	0.029	0.036	0.020
11	4	0.033	0.021	0.037	0.033	0.026	0.031	0.009	0.022	0.027	0.027
12	1	0.078	0.018	0.057	0.021	0.053	0.011	0.046	0.023	0.059	0.019
12	2	0.074	0.024	0.025	0.019	0.030	0.012	0.034	0.011	0.041	0.017
12	3	0.039	0.013	0.015	0.015	0.022	0.011	0.021	0.011	0.024	0.013
12	4	0.049	0.022	0.021	0.015	0.007	0.020	0.027	0.019	0.026	0.019
Mean		.038	0.026	0.038	0.022	0.037	0.019	0.038	0.021	0.038	0.022

Table 5b: Means and standard deviations of conductivity error (DC) for layers defined in Table 4.

C	X	DEPTH-1 AV	DEPTH-1 SD	DEPTH-2 AV	DEPTH-2 SD	DEPTH-3 AV	DEPTH-3 SD	DEPTH-4 AV	DEPTH-4 SD	VERT. AV AV	VERT. AV SD
4	1	0.097	0.074	0.049	0.029	0.028	0.024	0.037	0.017	0.053	0.042
4	2	0.080	0.081	0.041	0.035	-0.105	0.017	-0.103	0.021	-0.022	0.046
4	3	0.086	0.061	0.044	0.036	-0.219	0.010	-0.204	0.011	-0.073	0.036
4	4	0.118	0.062	0.062	0.033	0.024	0.019	0.038	0.016	0.060	0.037
5	1	0.050	0.060	0.032	0.017	-0.062	0.029	-0.154	0.016	-0.033	0.035
5	2	0.065	0.042	-0.107	0.019	-0.144	0.012	-0.134	0.012	-0.080	0.024
5	3	0.046	0.046	0.037	0.016	0.029	0.011	0.038	0.015	0.038	0.026
5	4	0.001	0.059	0.006	0.012	0.005	0.020	0.005	0.010	0.004	0.032
6	1	0.090	0.044	0.035	0.018	0.036	0.014	0.039	0.017	0.050	0.027
6	2	0.099	0.035	0.039	0.018	0.034	0.018	0.030	0.015	0.051	0.023
6	3	0.047	0.019	0.043	0.017	0.035	0.018	0.049	0.017	0.043	0.018
6	4	0.116	0.026	0.048	0.021	0.043	0.020	0.053	0.008	0.065	0.020
7	1	0.103	0.071	0.030	0.024	0.043	0.009	0.035	0.019	0.053	0.039
7	2	-1.035	0.077	-0.803	0.018	-0.734	0.009	-0.723	0.012	-0.824	0.040
7	4	0.123	0.077	0.042	0.022	0.029	0.012	0.026	0.014	0.055	0.041
8	1	0.061	0.049	0.028	0.022	-0.001	0.010	-0.017	0.020	0.018	0.029
8	2	0.073	0.047	0.018	0.026	0.012	0.009	-0.008	0.010	0.024	0.028
8	3	0.086	0.068	0.026	0.015	0.033	0.011	0.016	0.015	0.040	0.036
8	4	0.044	0.063	-0.045	0.024	-0.102	0.021	-0.112	0.021	-0.054	0.037
9	1	0.054	0.033	-0.038	0.018	-0.140	0.007	-0.169	0.008	-0.073	0.019
9	2	-0.432	0.041	-0.568	0.024	-0.488	0.016	-0.456	0.014	-0.486	0.026
9	3	-0.346	0.051	-0.490	0.024	-0.475	0.028	-0.456	0.021	-0.442	0.033
9	4	-1.341	0.033	-1.570	0.017	-1.518	0.024	-1.498	0.022	-1.482	0.025
10	1	-0.405	0.042	-0.440	0.012	-0.401	0.014	-0.381	0.009	-0.406	0.023
10	2	0.094	0.058	0.037	0.022	0.018	0.023	0.028	0.015	0.044	0.034
10	3	0.089	0.038	0.040	0.023	0.029	0.016	0.029	0.014	0.047	0.025
10	4	0.105	0.051	0.047	0.018	-0.145	0.024	-0.179	0.016	-0.043	0.031
11	2	0.020	0.041	0.047	0.022	0.024	0.014	0.019	0.027	0.027	0.028
11	3	0.016	0.024	-0.210	0.016	-0.249	0.013	-0.260	0.028	-0.176	0.021
11	4	-2.072	0.027	-1.012	0.021	-1.121	0.019	-1.125	0.021	-1.333	0.022
12	1	0.094	0.031	0.038	0.019	0.039	0.011	0.016	0.023	0.047	0.022
12	2	0.155	0.088	0.022	0.022	0.014	0.022	0.006	0.019	0.049	0.048
12	3	0.075	0.035	-0.017	0.022	-0.015	0.014	-0.033	0.011	0.003	0.022
12	4	0.083	0.040	-0.006	0.016	-0.025	0.010	-0.012	0.015	0.010	0.023
Mean		-0.102	0.053	-0.132	0.022	-0.161	0.017	-0.164	0.017	-0.140	0.031

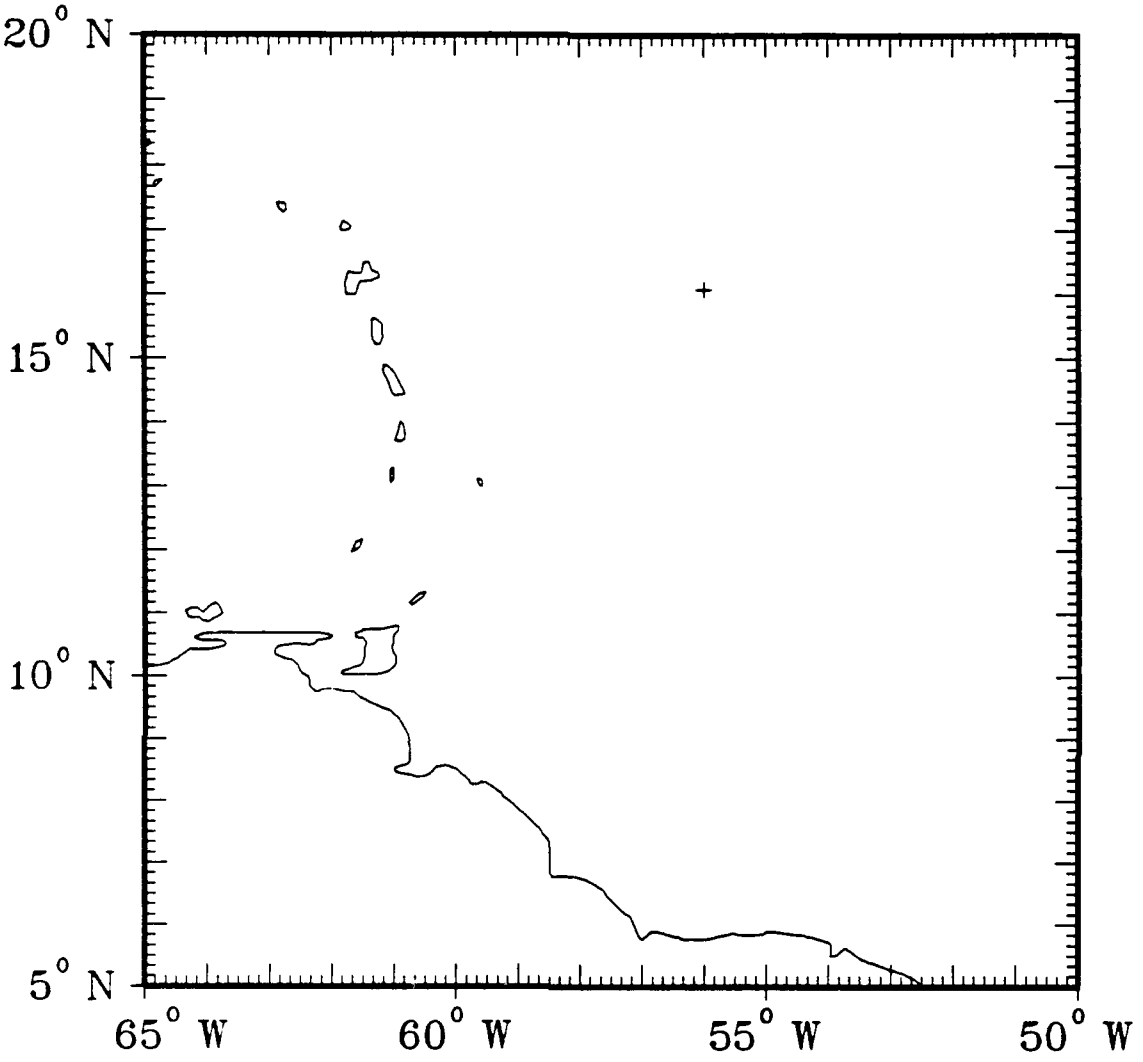

Figure 1. Map of region of operation; experiment location marked by +.

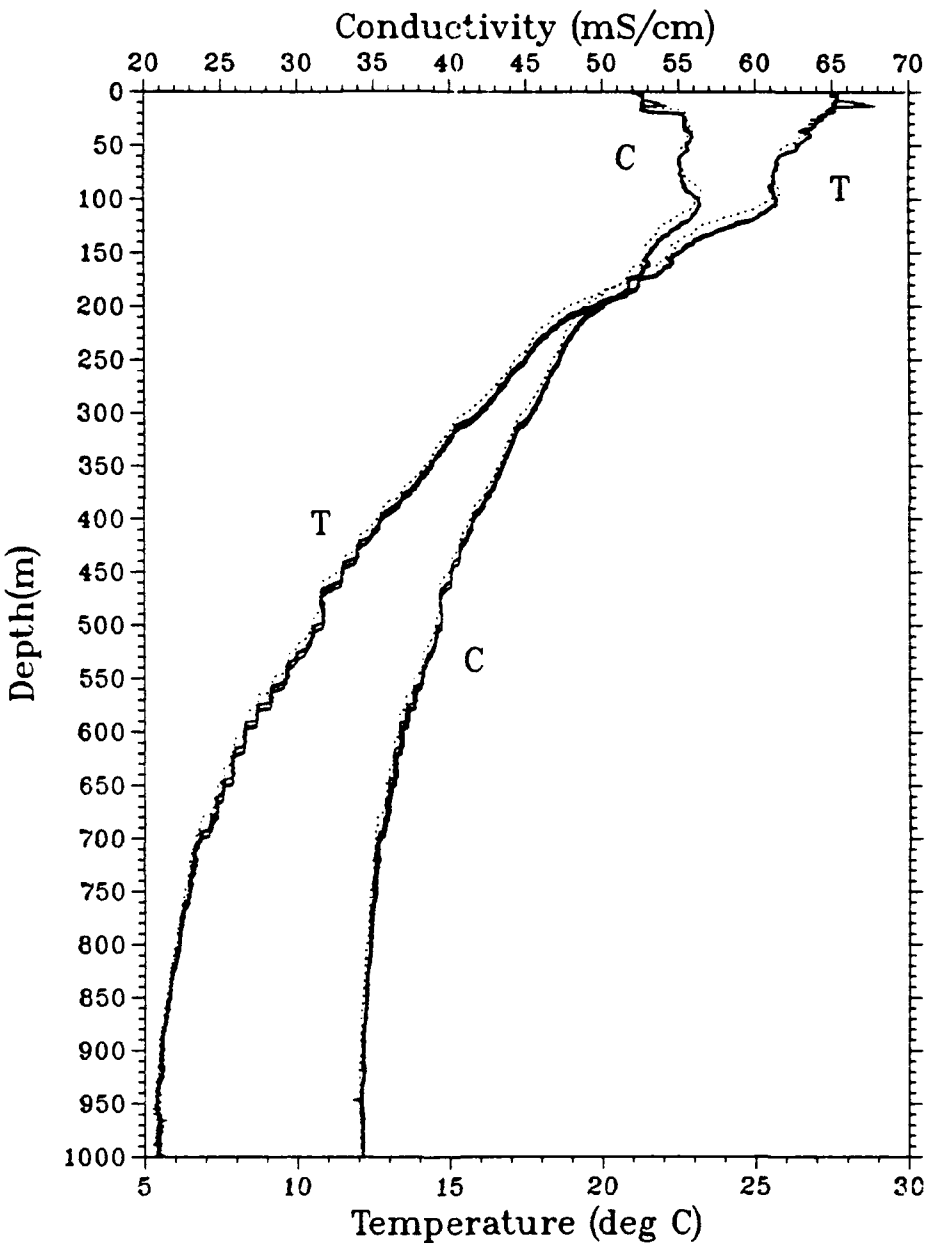

Figure 2. Profile plots of temperature and conductivity for CTD group 4. CTD data - dashed, XCTD data - solid.

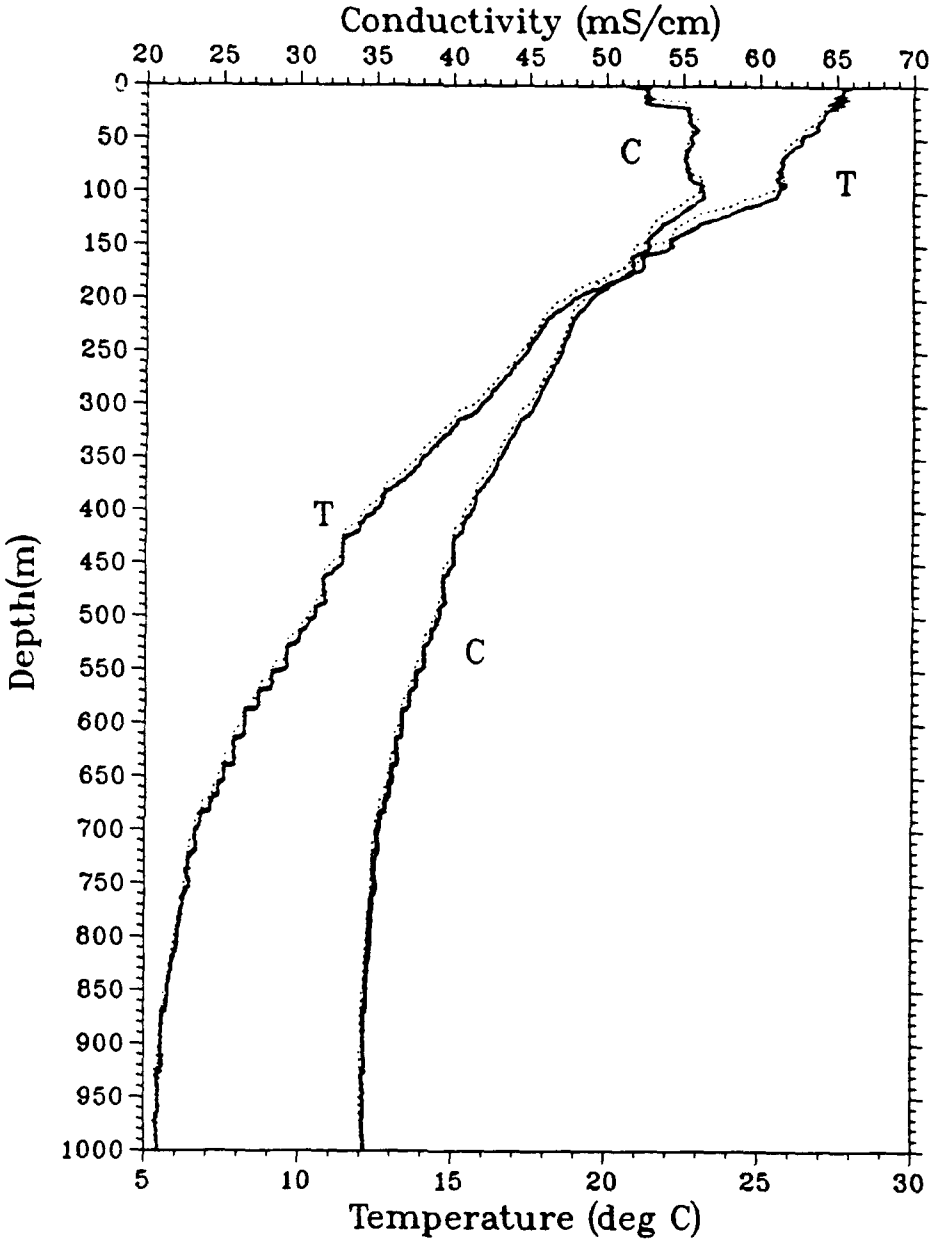

Figure 3. Profile plots of temperature and conductivity for CTD group 5. CTD data - dashed, XCTD data - solid.

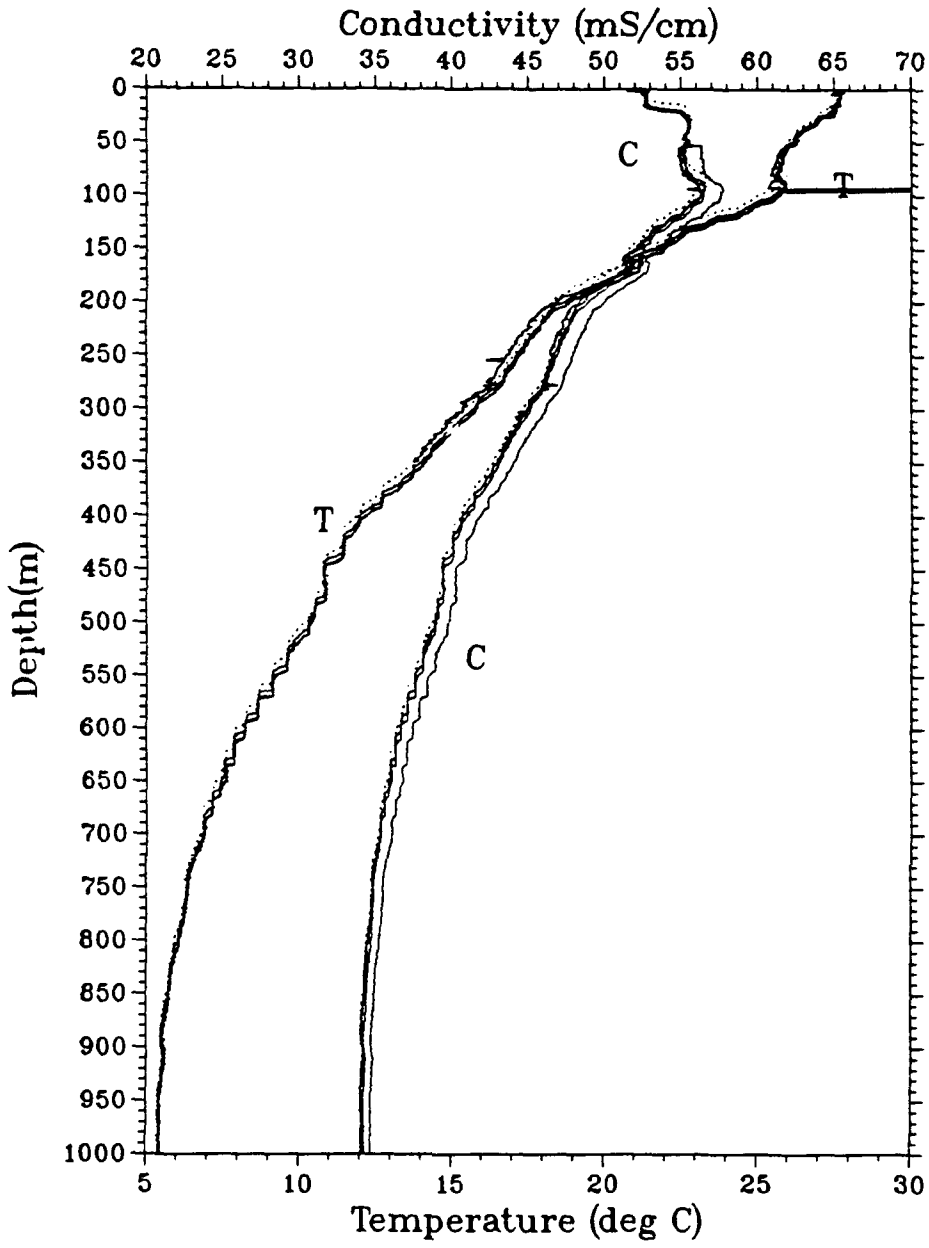

Figure 5. Profile plots of temperature and conductivity for CTD group 7. CTD data - dashed, XCTD data - solid.

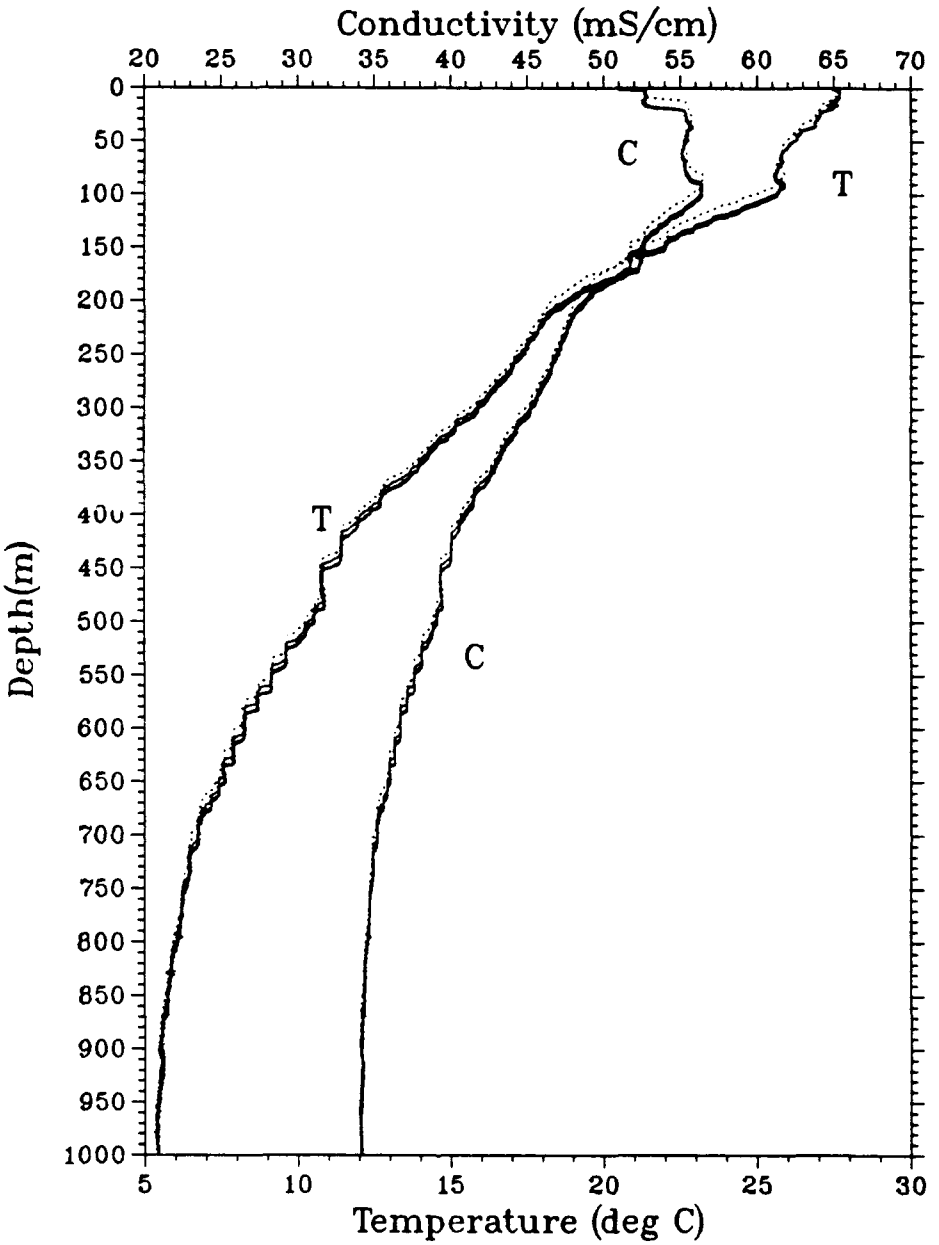

Figure 4. Profile plots of temperature and conductivity for CTD group 6. CTD data - dashed. XCTD data - solid.

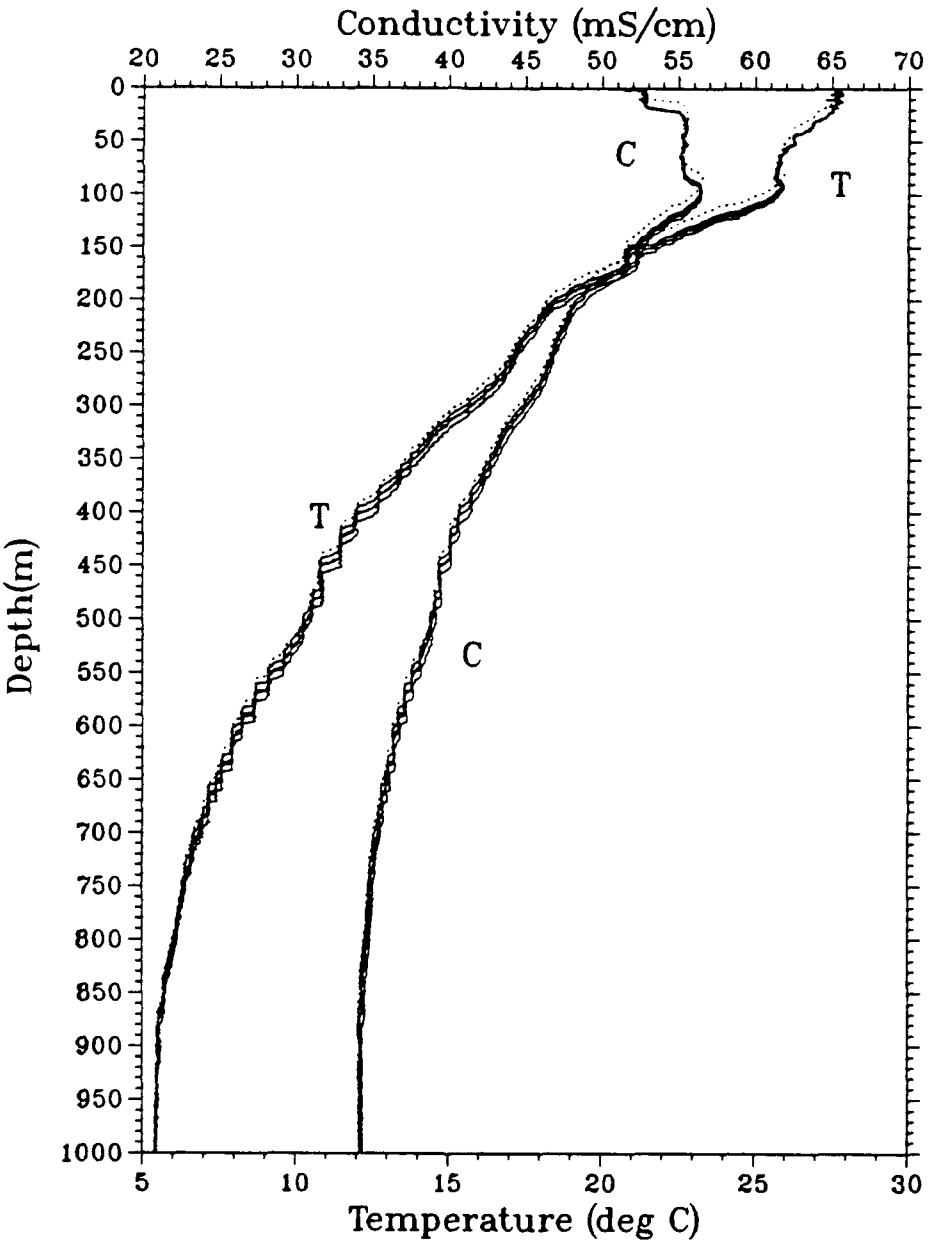

Figure 6. Profile plots of temperature and conductivity for CTD group 8. CTD data - dashed, XCTD data - solid.

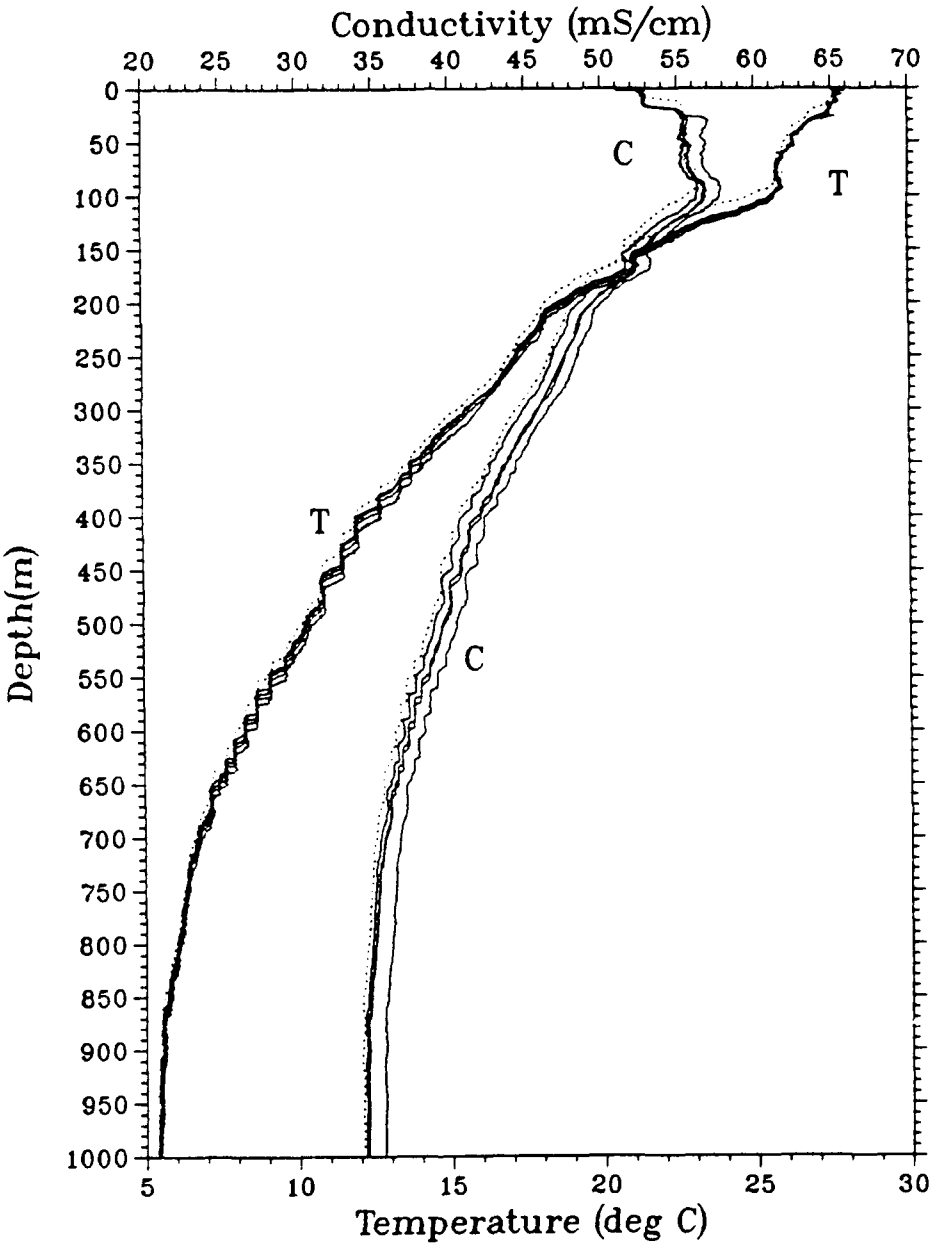

Figure 7. Profile plots of temperature and conductivity for CTD group 9. CTD data - dashed, XCTD data - solid.

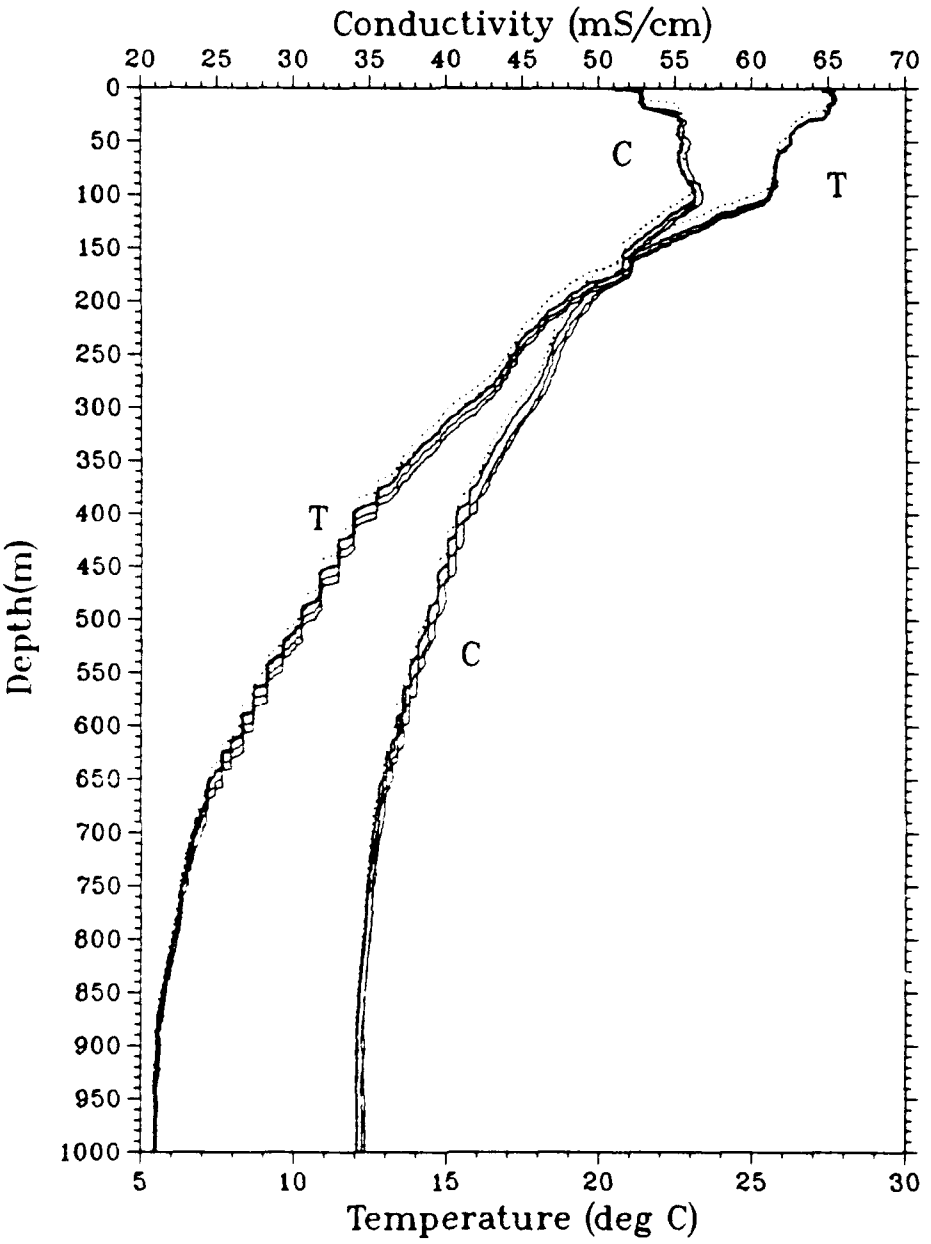

Figure 8. Profile plots of temperature and conductivity for CTD group 10. CTD data - dashed, XCTD data - solid.

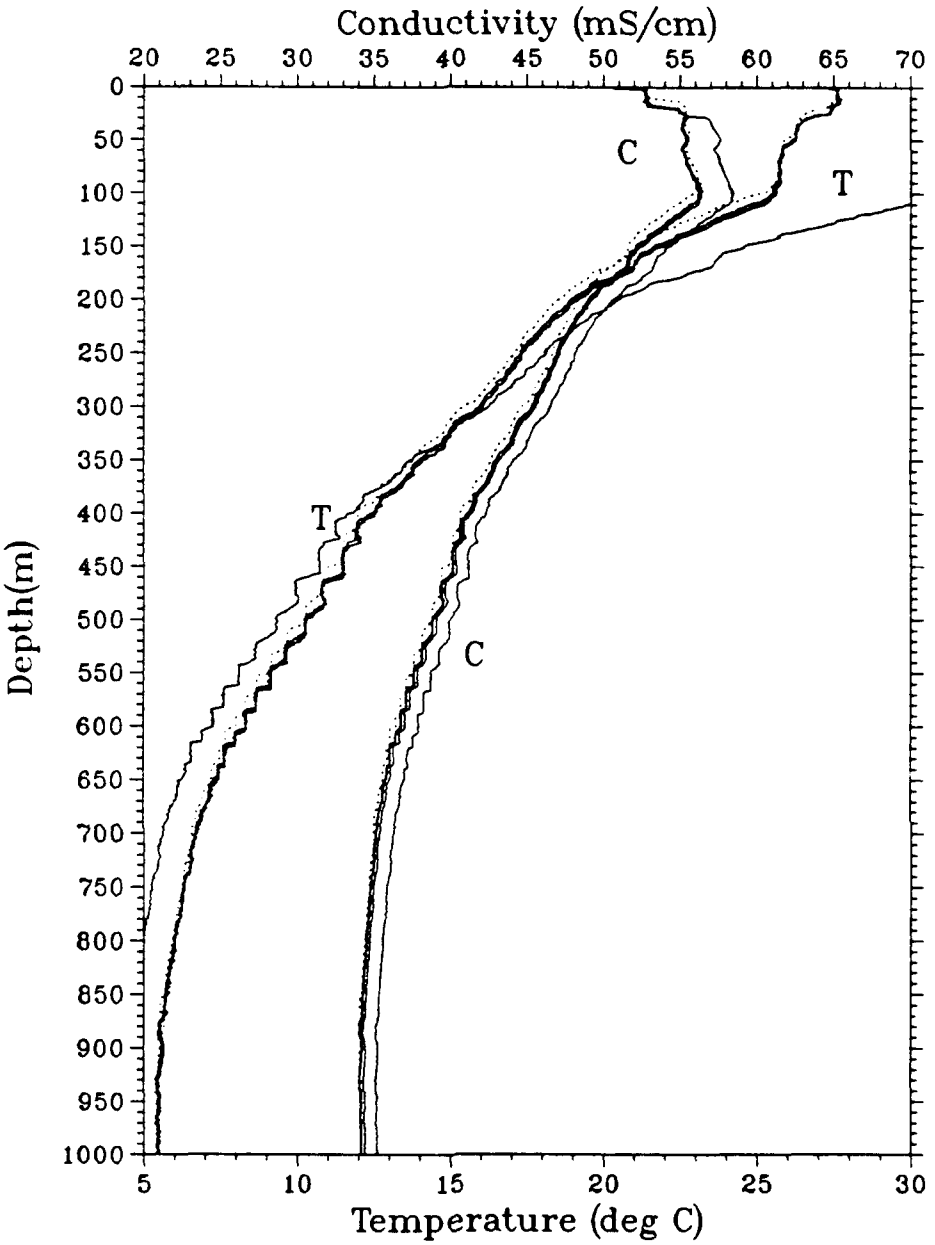

Figure 9. Profile plots of temperature and conductivity for CTD group 11. CTD data - dashed, XCTD data - solid.

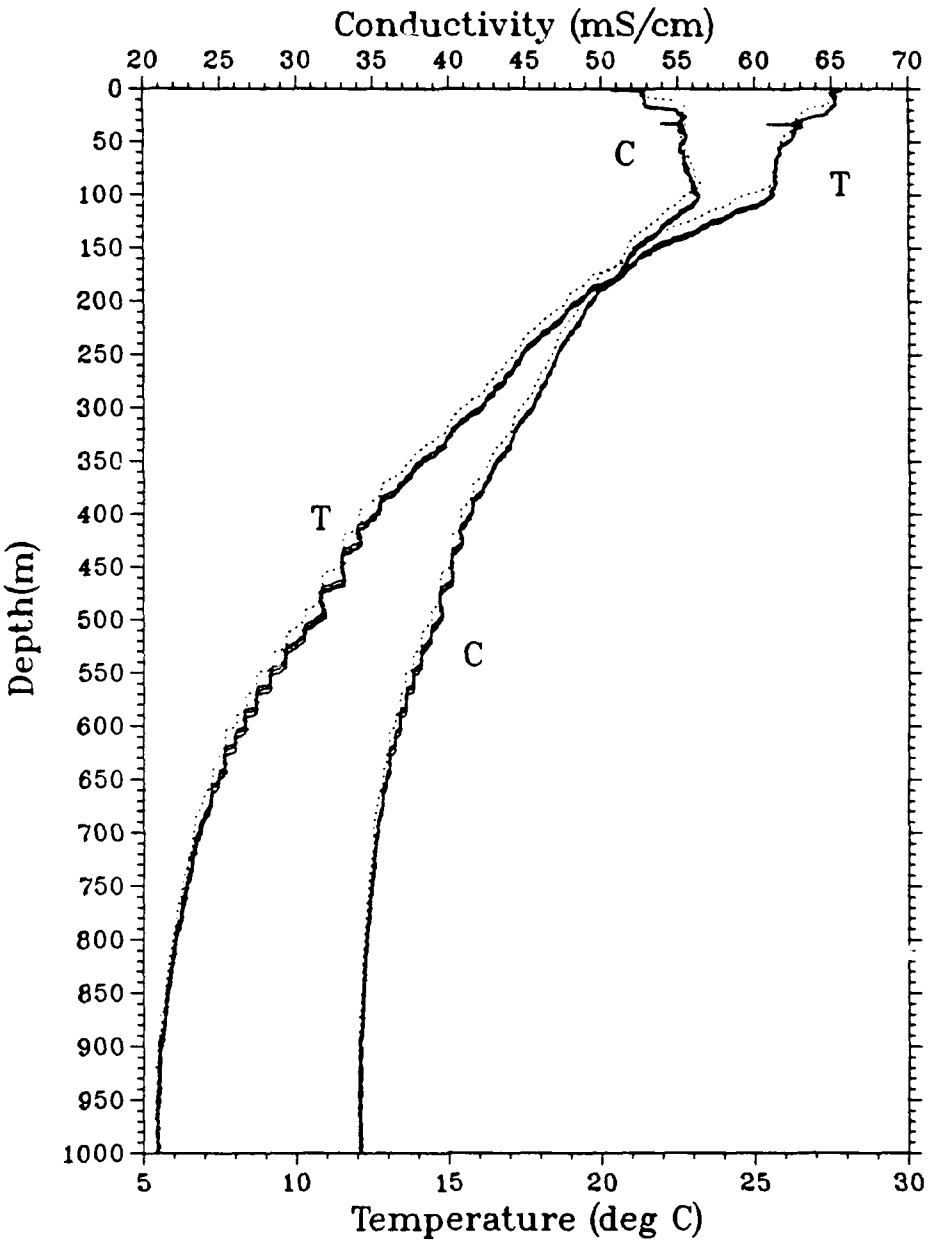

Figure 10. Profile plots of temperature and conductivity for CTD group 12. CTD data - dashed, XCTD data - solid.

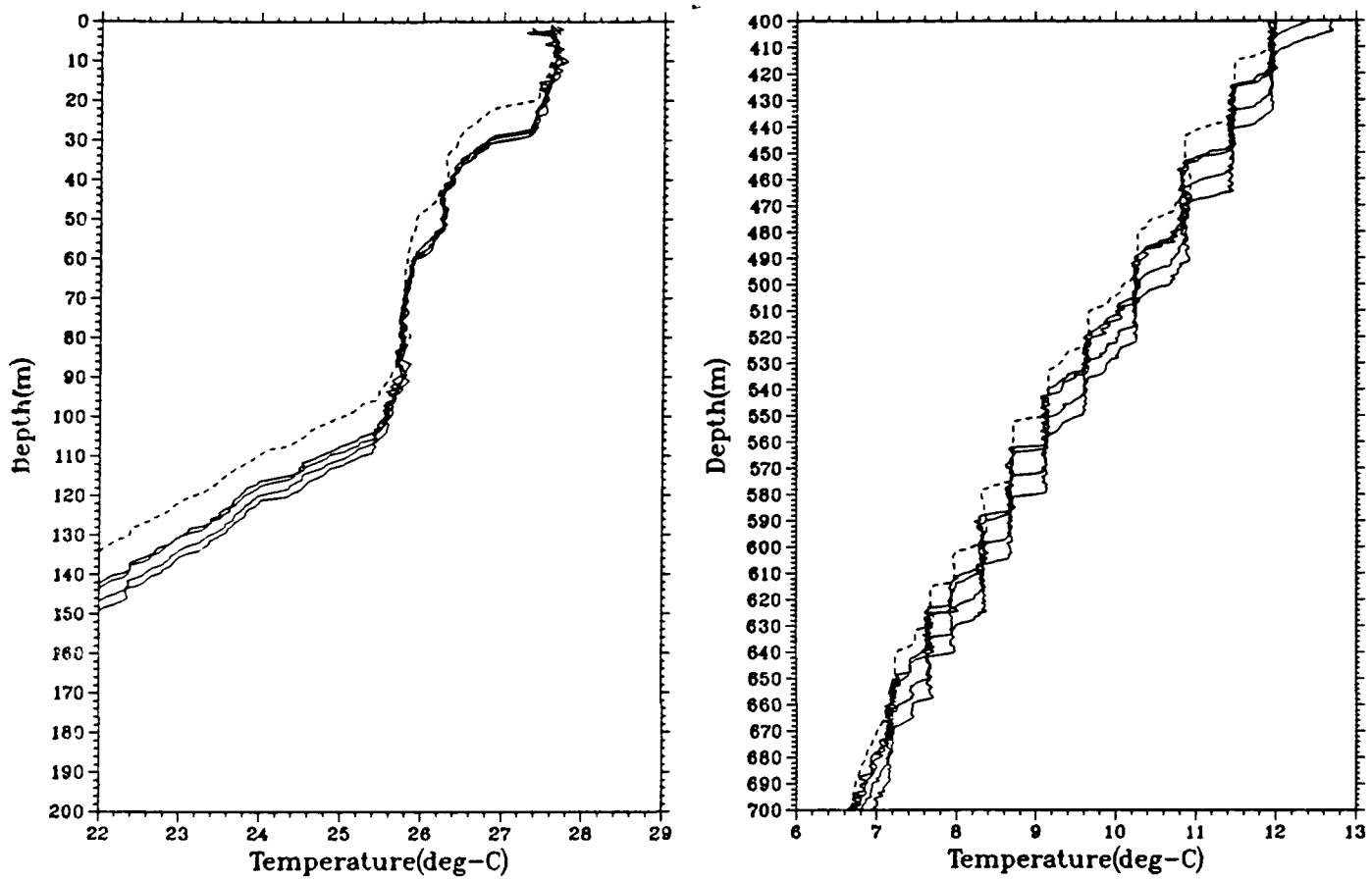

Figure 11. Expanded profile plots of temperature for (a) 0 - 200 m, and (b) 400 - 700 m. CTD data - dashed, XCTD data - solid. XCTD depths are based on original equation.

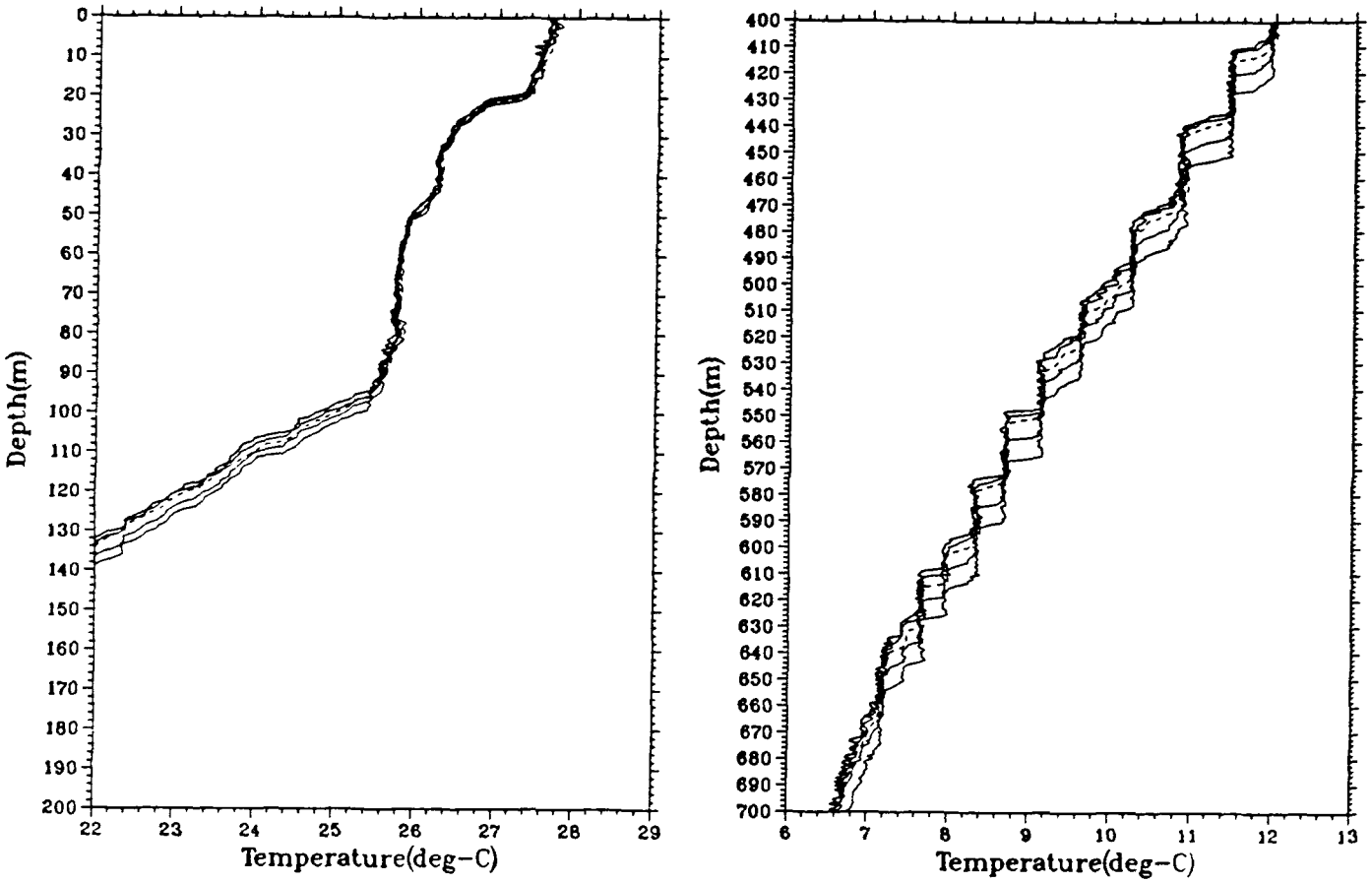

Figure 12. Expanded profile plots of temperature for (a) 0 - 200 m, and (b) 400 - 700 m. CTD data - dashed, XCTD data - solid. XCTD depths are recalculated with single set of coefficients (Method-I, Case-I coefficients).

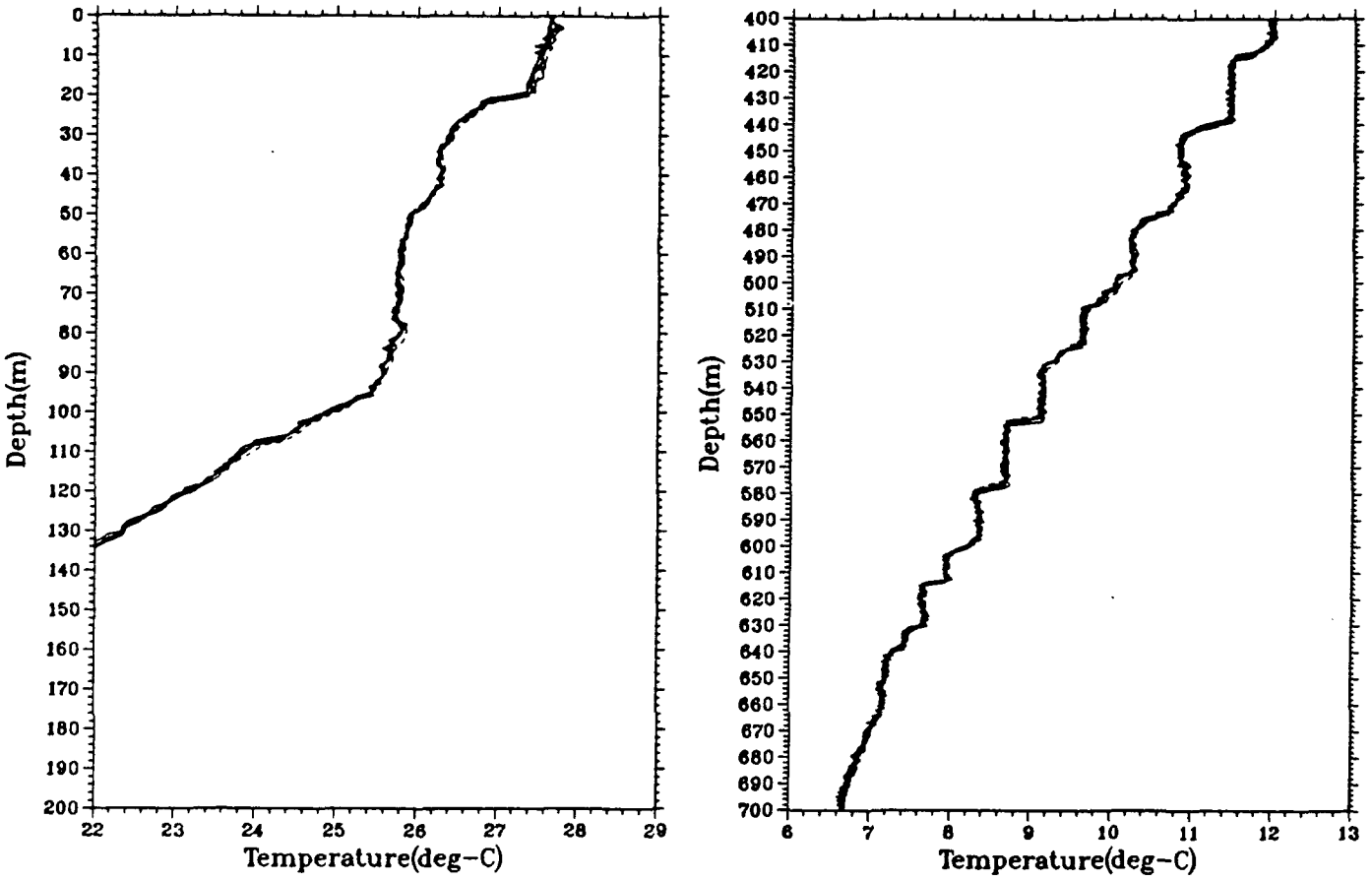

Figure 13. Expanded profile plots of temperature for (a) 0 - 200 m, and (b) 400 - 700 m. CTD data - dashed, XCTD data - solid. XCTD depths are recalculated with individually determined coefficients (Method-II, Case-I).

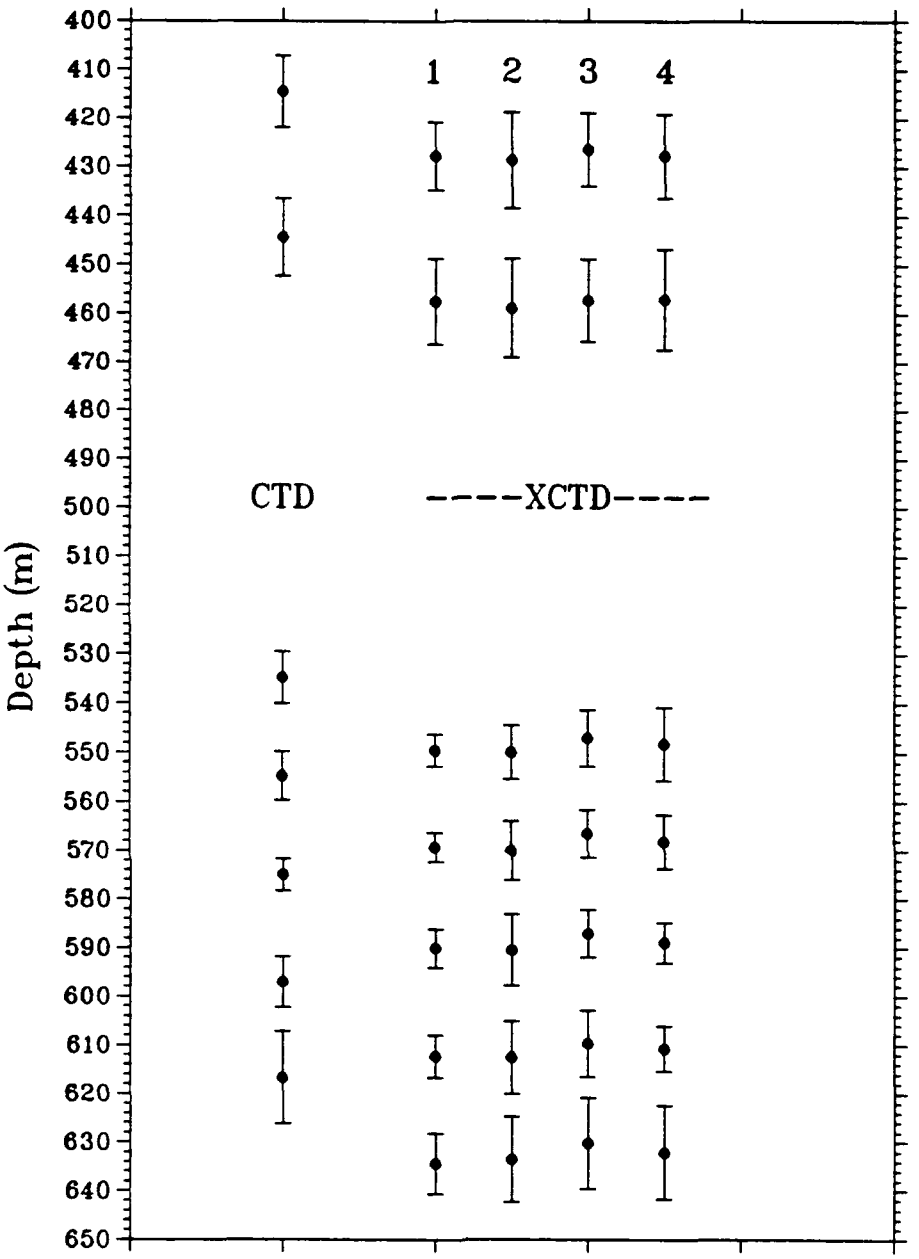

Figure 14. Temporal means and standard deviations (error bars) of feature depths for CTD and XCTD data. The latter were calculated separately for each launcher-acquisition system (numbered 1-4). Features are the seven steps in the deep interval (400 - 700 m).

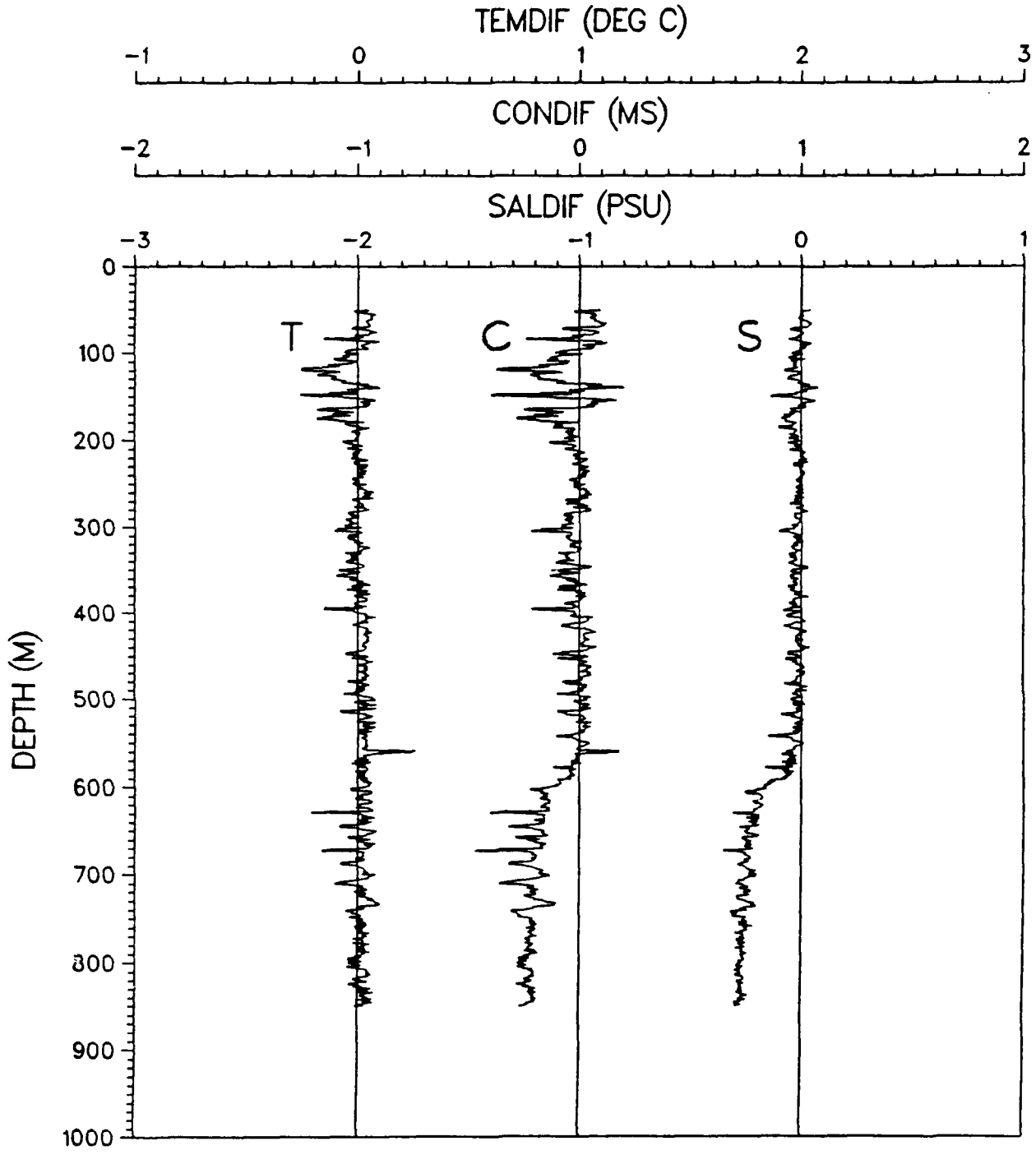

Figure 15. Sample profile plots of CTD-XCTD differences in temperature, conductivity and salinity (for XCTD 005015).

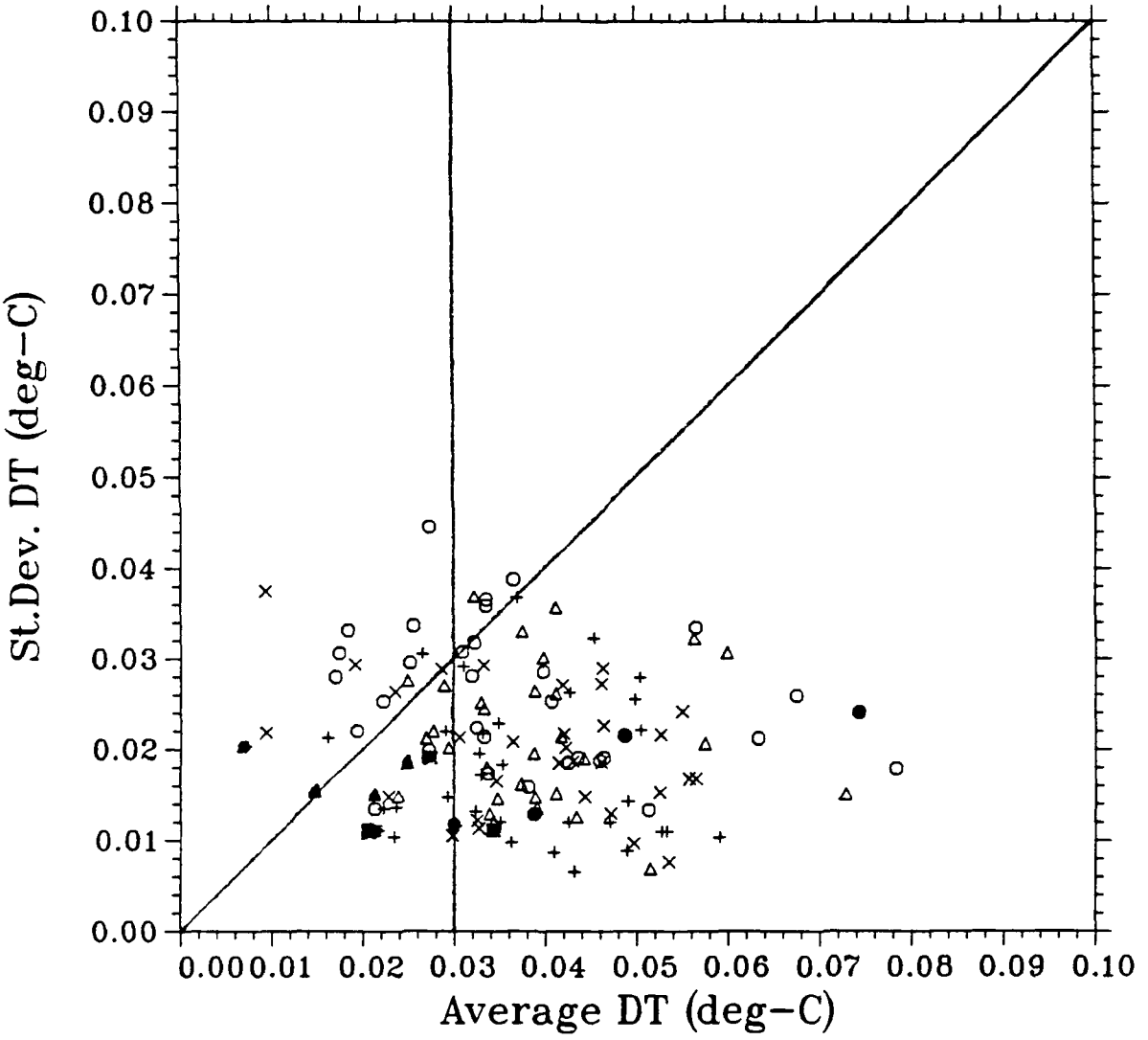

Figure 16. Layer statistics of CTD-XCTD temperature differences (DT). Abscissa is layer-average DT, ordinate is layer-standard deviation of DT. Layer-depths are denoted by: near-surface - circles, about 450 m - triangles, about 575 m - plusses, about 600 m - Xs. Foam-filled probes are denoted by shaded symbols. The diagonal line indicates equality of mean and standard deviation. The vertical line indicates the manufacturer's tolerance.

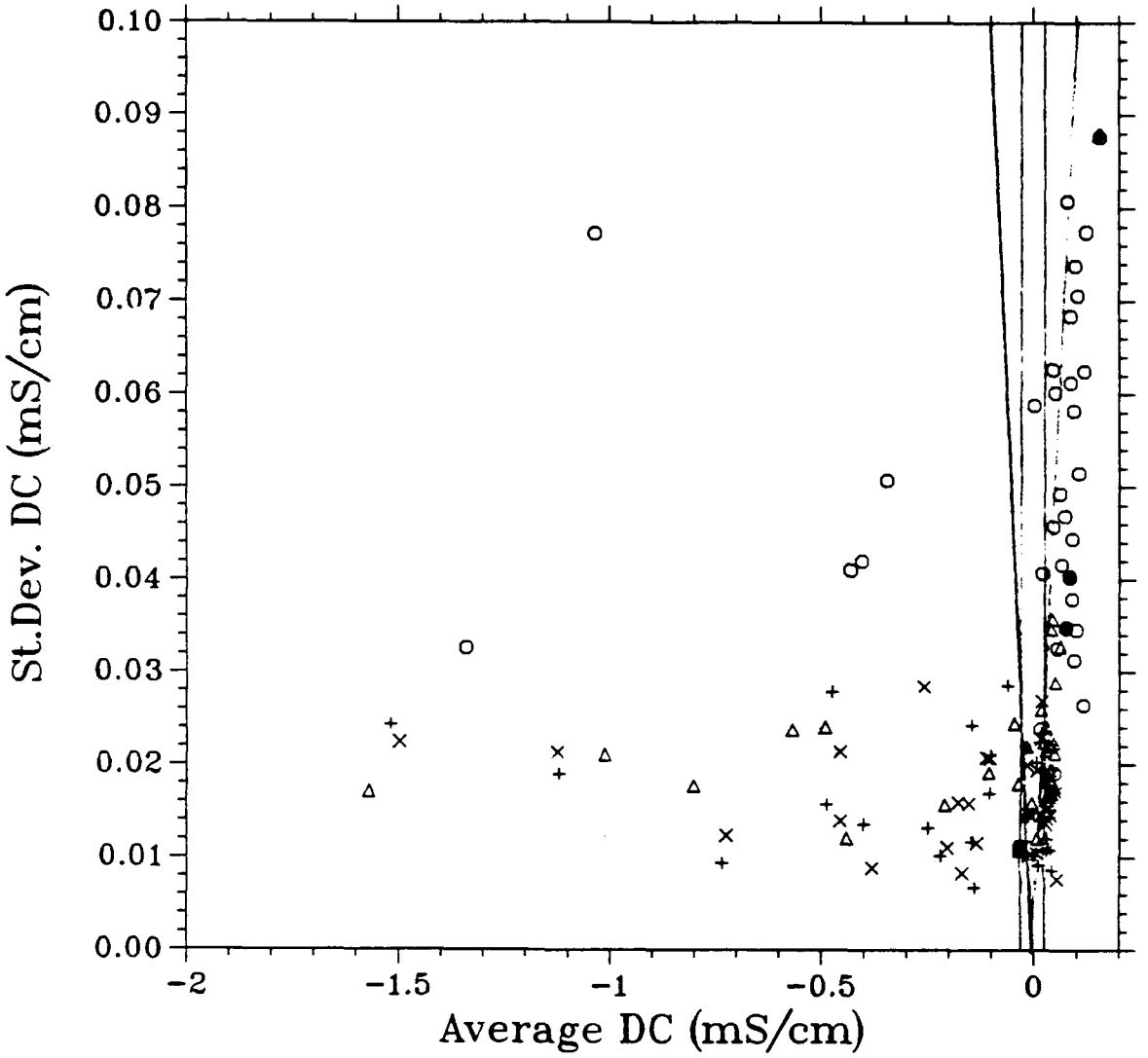

Figure 17. Layer statistics of CTD-XCTD temperature differences (DT). Abscissa is layer-average DT, ordinate is layer-standard deviation of DT. Layer-depths are denoted by: near-surface - circles, about 450 m - triangles, about 575 m - plusses, about 600 m - Xs. Foam-filled probes are denoted by shaded symbols. The diagonal lines indicate equality of mean and standard deviation. The vertical lines indicate the manufacturer's tolerance.

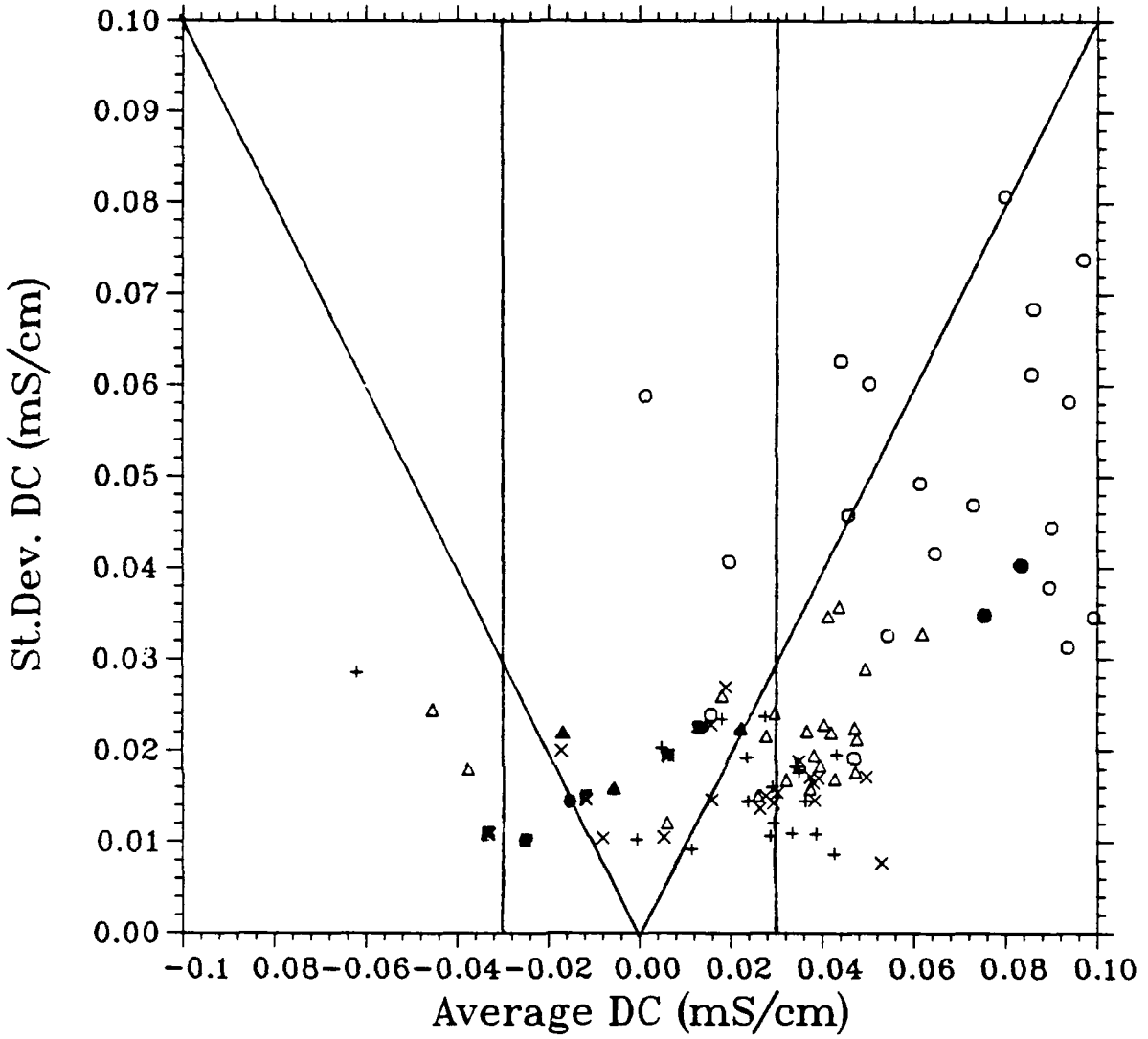

Figure 18. Layer statistics of CTD-XCTD conductivity differences (DC). Abscissa is layer-average DC, ordinate is layer-standard deviation of DC. Layer-depths are denoted by: near-surface - circles, about 450 m - triangles, about 575 m - plusses, about 600 m - Xs. Foam-filled probes denoted by shaded symbol. The diagonal lines indicate equality of mean and standard deviation, vertical lines indicate the manufacturer's tolerance. This plot is the same as Figure 17, with a larger scale.

DISTRIBUTION LIST

Sippican Corporation
7 Barnabas Road
Marion, MA 02738-1499
Attn: Bruce Dalton

Sparton of Canada
99 Ash Street
London, Ontario, Canada NGA 4N2
Attn: Bruce Eidsvik

Office of the Oceanographer of the Navy
CNO OP-096
U.S. Naval Observatory Bldg-1 Room K
34th & Massachusetts Ave N.W.
Washington, D.C. 20392-1800
Attn: CDR Perdue

Office of Naval Research
800 North Quincy St
Arlington, VA 22217
Attn: Environmental Sciences

Naval Oceanographic Office
Stennis Space Center, MS 39529
Attn: Vance Sprague, Code OP

NOARL
Code 300
Code 311
Code 330
Code 331
Code 125L (10)
Code 125P

REPORT DOCUMENTATION PAGE

Form Approved
OBM No. 0704-0188

1. Agency Use Only *(Leave blank).*	2. Report Date.	3. Report Type and Dates Covered.
	September 1990	Final

4. Title and Subtitle.
XCTD Test: Reliability and Accuracy Study (XTRAS)

5. Funding Numbers.

Program Element No.	604704N/603704N
Project No.	R1740/R0118
Task No	300
Accession No.	DN259042

6. Author(s).
Z. R. Hallock and W. J. Teague

7. Performing Organization Names(s) and Address(es).
Naval Oceanographic and Atmospheric Research Laboratory
Ocean Science Directorate
Stennis Space Center, Mississippi 39529-5004

8. Performing Organization Report Number.
NOARL Technical Note 69

9. Sponsoring/Monitoring Agency Name(s) and Address(es).
Naval Oceanographic and Atmospheric Research Laboratory
ASW Oceanography Office
Stennis Space Center, Mississippi 39529-5004

10. Sponsoring/Monitoring Agency Report Number.
NOARL Technical Note 69

11. Supplementary Notes.

12a. Distribution/Availability Statement.
Approved for public release; distribution is unlimited.

12b. Distribution Code.

13. Abstract *(Maximum 200 words).*

In May-June 1990 a test and evaluation of the newly developed XCTD (expendable conductivity, temperature, depth) probe was conducted in a region northeast of Barbados, where ideal conditions exist for such a test. Thirty-six XCTD probes were launched concurrently with nine CTD casts for intercomparison. The existing fall-rate equation (FRE) was found to be inadequate and new coefficients were computed by regression using the CTD data. After recalculating XCTD depths, simultaneous drops show significant probe-to-probe difference, indicating a nonsystematic difference in (primarily) the linear term in the FRE for each probe. Examination of temperature and conductivity shows a significant systematic offset of the XCTDs relative to the CTD, suggesting a calibration error. In addition, many of the probes exhibited huge, positive conductivity excursions indicative of conductivity cell malfunction. Sippican Ocean Systems has indicated that the cell malfunctions and the calibration problems are correctable, but it is not clear if there is a solution for the residual depth error.

14. Subject Terms.
(U) Physical Oceanography, (U) XCTD, (U) Expendable Sensors

15. Number of Pages.
33

16. Price Code.

17. Security Classification of Report.	18. Security Classification of This Page.	19. Security Classification of Abstract.	20. Limitation of Abstract.
Unclassified	Unclassified	Unclassified	SAR